Stress concentration factors of cold-formed stainless steel tubular X-joints

Ran Feng [a] and Ben Young [b,*]

[a] *School of Civil Engineering, Hefei University of Technology, Hefei, Anhui, China*

[b] *Department of Civil Engineering, The University of Hong Kong, Pokfulam Road, Hong Kong*

Abstract

This paper describes experimental and numerical investigations on stress concentration factors (SCFs) of cold-formed stainless steel square and rectangular hollow section (SHS and RHS) tubular X-joints. Both high strength stainless steel (duplex and high strength austenitic) and normal strength stainless steel (AISI 304) specimens were investigated. The SCFs were experimentally determined under static loading by measuring the strains at typical hot spot locations using strip strain gauges. The corresponding finite element analysis was performed to simulate the non-uniform stress distribution along the brace and chord intersection region. Good agreement between the experimental and finite element analysis results was achieved. Therefore, an extensive parametric study was then carried out by using the verified finite element model to evaluate the effects of the SCFs of cold-formed stainless steel tubular X-joints. The SCFs at the hot spot locations obtained from the experimental investigation and parametric study were compared with those calculated using the design formulae given in the CIDECT for carbon steel tubular X-joints. It is shown from the comparison that the design rules for the SCFs specified in the CIDECT are generally quite unconservative for cold-formed stainless steel tubular X-joints. In this study, a unified design equation for the SCFs of cold-formed stainless steel tubular X-joints is proposed. The proposed design equation was based on the CIDECT design equation for carbon steel tubular X-joints. It is shown that the SCFs calculated from the proposed unified design equation are generally in agreement with the values predicted from finite element analysis.

Keywords: Cold-formed stainless steel; High strength; Hot spot strain (HSSN); Hot spot stress (HSS); Rectangular hollow section (RHS); Square hollow section (SHS); Strain concentration factor (SNCF); Stress concentration factor (SCF); Tubular joint

* Corresponding author. Tel.: +852 2859 2674; fax: +852 2559 5337.
E-mail address: young@hku.hk (B. Young).

1. Introduction

Cold-formed welded tubular joints made of square hollow section (SHS) and rectangular hollow section (RHS) are widely used in onshore and offshore structures. These tubular joints are often subjected to cyclic loading and fail by fatigue. It is very important to investigate the fatigue behaviour of welded tubular joints, since this type of failure is normally caused by loading applied repeatedly and the loads could be small. The fatigue failure is an accumulate process and the corresponding fatigue loads are much lower than the ultimate loads resulted from static failure. Hence, the design procedures related to the static failure criterion are inapplicable to the fatigue failure problem. The most commonly used method to assess the fatigue life of welded tubular joints is the hot spot stress (HSS) method, which is also called geometric stress method. This method estimates the fatigue resistance of welded tubular joints based on the HSS rather than the nominal stress.

The HSS ranges at the so-called hot spot locations can be determined by either experimental techniques using special strain gauges or sophisticated three dimensional finite element analyses. These two approaches, however, are not feasible for engineering designers. Thus, an important parameter called stress concentration factor (SCF) was introduced in the fatigue design, which is the ratio between the HSS at the joint intersection area and the nominal stress obtained from the applied load that causes this HSS.

Currently, there is no design equation to calculate the SCF for cold-formed stainless steel tubular joints. The design equations for the calculation of SCFs given in the CIDECT Design Guide No. 8 [1] are only applicable to carbon steel tubular joints. Therefore, one of the aims of this study is to propose design equation for the calculation of SCFs for cold-formed stainless steel tubular X-joints. Cold-formed stainless steel tubular X-joints were tested. In addition, finite element analysis was performed and an extensive parametric study was carried out. The data obtained from this study were used to compare with the SCFs predicted using the proposed design equation.

2. Hot spot stress (HSS) method

2.1. General

Experimental stress analysis and finite element method (FEM) are commonly used to estimate

the SCFs of welded tubular joints. Many parametric formulae based on either strain gauge measurements or FEM have been reported for different types of welded tubular joints subjected to different loading cases. Toprac et al. [2] carried out one of the early experimental works on the fatigue behaviour of tubular joints. It was concluded from the test results that the stress concentration was an important factor and the point of crack initiation at the weld toe occurred on the highest stress. Kuang et al. [3] derived SCF formulae based on thin shell finite element models, which pioneered the numerical analysis method for the determination of the SCFs of tubular joints. The middle surface of the member wall thickness was modelled and the weld element was omitted at the joint intersection. Thus, the comparison of the SCFs obtained from the finite element analysis with the experimental results showed a difference of 20% and the predicted SCFs of the KT-joints were four times higher. Gibstein [4] derived SCF formulae for T- and Y-joints based on finite element analyses. It was commented that the thin shell theory was inadequate for the three-dimensional stress condition at the joint intersection. Romeijn et al. [5] established guidelines on the determination of the SCFs of tubular joints on several important aspects numerically. For the finite element analysis, the 20-noded solid element with the SCFs defined at the weld toe was commented to be the most accurate finite element model. The stresses perpendicular to the weld toes were suggested for the determination of the SCFs. The combination of linear and parabolic curves was the recommended extrapolation procedure for the nonlinear stress gradients. It was finally suggested that compensation moments should be applied to the chord ends to eliminate the effect of the boundary conditions on the SCFs. Additionally, the effect of chord member loads due to axial force, in-plane and out-of-plane bending on the SCFs of T- and Y-joints was also studied. It should be noted that the aforementioned investigations focused on carbon steel tubular joints rather than stainless steel tubular joints.

Macdonald and Haagensen [6] studied the fatigue behaviour of welded aluminum RHS T-joints based on both fatigue tests and finite element analysis. Appropriate SCFs were determined from strain gauge measurements in the experimental investigation and the validated finite element modelling. Parametric equations for the prediction of the SCFs of aluminum RHS T-joints were proposed. The HSS method has also been discussed in many fatigue design guidelines. The definition of HSS, however, is still under debate.

2.2. Stress concentration factor (SCF) and strain concentration factor (SNCF)

In most fatigue design guidelines, HSS and SCF are usually presented. They are actually determined based on the corresponding strains, which show a certain degree of advantages compared to the stresses (van Wingerde et al. [7]):

- The hot spot strain (HSSN) can be easily measured by the specially designed strain gauges, whereas the HSS should be calculated based on the relative strain components.
- Fatigue is a strain-based phenomenon rather than a stress-driven mechanism. The HSS can not significantly exceed the yield stress of structural members.

Therefore, the HSS and SCF can then be predicted in terms of the corresponding HSSN and SNCF.

2.3. Type of stress for the determination of SCF

Fatigue design procedures for carbon steel tubular joints are available in the International Institute of Welding Subcommission XV-E [8], Department of Energy [9] and Eurocode 3 part 1.9 [10]. The principal stress was recommended in these design guidelines to be used for the determination of SCF. In some other fatigue design codes, such as the American Welding Society [11], American Petroleum Institute [12] and CIDECT Design Guide No. 8 [1], however, the stress perpendicular to the weld toe was employed in the HSS method. The stress perpendicular to the weld toe rather than the principal stress is preferable due to the following reasons (van Wingerde et al. [7]):

- Strains perpendicular to the weld toe can be easily measured by simple strain gauges instead of complex strain gauge rosettes, which is specially designed for principal strains.
- The closer the position to the weld toe, the smaller the difference between the principal stress and stress perpendicular to the weld toe.
- Among stress components, only stresses perpendicular to the weld toe are enlarged by stress concentrations from weld shape and relative tubular members.
- In the extrapolation method to exclude the effects of welding fabrication, all strain components of the principal strains need to be extrapolated, which makes the procedure quite complicated.
- The direction of the principal stress is different for different loading cases, which makes the superposition technique for combined loading difficult.

2.4. Hot spot location

The SCF may vary around the intersection region of the welded tubular joints. Several fixed lines *A* to *E* representing so-called hot spot locations were chosen for the determination of the SCFs, as shown in Fig. 1. These fixed lines for SHS and RHS tubular joints are recommended in the CIDECT Design Guide No. 8 [1]. The HSS determined at the hot spot locations may underestimate the true HSS if the direction of the principal stress deviates from those fixed lines, especially if the stress concentration is less pronounced. A minimum SCF equaled 2.0 was then recommended. This recommendation is also applicable to the full width welded tubular joints and tubular joints whose SCFs significantly depend on the weld shapes.

2.5. Extrapolation method

The stress concentrations related to the welding fabrication and local condition of the weld toe will not be taken into account in the HSS method since they can not be easily determined. Therefore, an extrapolation procedure for strain distribution was recommended in many fatigue design guidelines to estimate the HSSN at the weld toe based on the geometric strains outside the brace and chord intersection region, which are significantly affected by the welding fabrication. Two extrapolation methods namely linear and quadratic extrapolation are commonly used for the determination of HSSN, as shown in Fig. 2. It was proposed in the CIDECT Design Guide No. 8 [1] that the linear extrapolation method is applicable to circular hollow section (CHS) tubular joints, while the quadratic extrapolation method can be used for SHS and RHS tubular joints due to the strong nonlinear strain distribution.

In addition to the linear and nonlinear extrapolation methods, the determination of extrapolation region is also quite important. In the early US practice for offshore structures, the hot spot was assumed to be located at the weld toe. The American Welding Society [11] and American Petroleum Institute [12] defined the HSS to be obtained from the strain gauges placed within 6 mm to $0.1\sqrt{rt}$ of the weld toe, in which r and t are the radius and thickness of relative tubular members. In the European Coal and Steel Community (ECSC) method [13], a value of $0.2\sqrt{rt}$ to $0.65\sqrt{rt}$ of the weld toe, with a minimum distance of 4 mm was used for the strain extrapolation. In the Det Norske Veritas (DNV) method [14], a value of 0.25t, with a minimum distance of 4 mm

was recommended as the extrapolation region. In the current fatigue design of the CIDECT Design Guide No. 8 [1], the extrapolation region for the strain distribution was also defined. For linear extrapolation method, two data points on the strain distribution curve will be used for the extrapolation. The first point was recommended to be 0.4*t* from the weld toe, with a minimum distance of 4 mm. The second point was taken to be 0.6*t* from the first data point, in which *t* is the wall thickness of tubular members whose strain distribution was extrapolated. For quadratic extrapolation method, a minimum of three strain gauges are required for the extrapolation. The first point was also 0.4*t* from the weld toe, with a minimum distance of 4 mm. The second point was taken to be 0.6*t* from the first data point. The third point was taken to be 1.0*t* from the first data point, in which *t* is the wall thickness of tubular members whose strain distribution was extrapolated. By means of least squares method, a quadratic curve fitting through all data points was formed. The quadratic SCF can then be obtained.

2.6. Purpose of this study

The previous investigations on the determination of the SCFs were mainly focused on carbon steel tubular joints. There is little research being carried out for cold-formed stainless steel tubular connections. With the rapid development of cold-formed stainless steel structures, the SCFs of cold-formed stainless steel tubular joints need to be investigated for fatigue design. It is well known that the mechanical properties of stainless steel sections are clearly different from those of carbon steel sections. Stainless steel sections have a rounded stress-strain curve with no yield plateau and low proportional limit stress compared to carbon steel sections. Hence, the fatigue design criteria of carbon steel tubular joints may not be applicable to the stainless steel tubular joints. To facilitate the use of stainless steel tubular connections, design guidelines should be provided for tubular joints subjected to fatigue loading.

This paper focuses on the SCFs of cold-formed stainless steel SHS and RHS tubular X-joints. Both high strength stainless steel (duplex and high strength austenitic) and normal strength stainless steel (AISI 304) specimens were investigated. The design guidelines given in the CIDECT Design Guide No. 8 [1] for carbon steel tubular joints were used in this study for stainless steel tubular joints. The SCFs at typical hot spot locations were presented in this paper.

3. Experimental investigation

3.1. General

The determination of SCF of welded tubular X-joints is depending mainly on the following: (1) the brace to chord width ratio ($\beta = b_1/b_0$); (2) the brace to chord thickness ratio ($\tau = t_1/t_0$); and (3) the chord width to thickness ratio ($2\gamma = b_0/t_0$). Tests were performed by applying axial compression force to the brace members using different values of β ranged from 0.5 to 1.0 (full width joint); τ from 0.5 to 1.5, and 2γ from 10 to 50. It should be noted that the parameters of τ and 2γ are beyond the validity range of most current design guidelines for SCF of welded tubular connections, in which $\tau \leq 1.0$ and $12.5 \leq 2\gamma \leq 25$.

3.2. Test specimens

The specimens were cold-rolled from austenitic stainless steel type AISI 304 (EN 1.4301), high strength austenitic (HSA) and duplex (EN 1.4462) stainless steel sheets. The stainless steel type AISI 304 is considered as normal strength material, whereas the HSA and duplex are considered as high strength material. The duplex stainless steel tubes are 40×40×2 and 140×80×3 having the measured 0.2% tensile proof stresses of 707 and 486 MPa, respectively; the high strength austenitic (HSA) stainless steel tubes are 150×150×6 and 200×110×4 having the measured 0.2% tensile proof stresses of 497 and 503 MPa, respectively; the normal strength stainless steel (AISI 304) tubes are 40×40×2 and 40×40×4 having the measured 0.2% tensile proof stresses of 447 and 565 MPa, respectively. It should be noted that the 0.2% tensile proof stresses of the stainless steel tubes were obtained from the tensile coupon tests based on the fabricated specimens after cold-forming. The process of cold-forming on square and rectangular hollow sections (SHS and RHS) by cold-working produces remarkable enhancement of the material properties. Hence, more economical designs can be achieved by taking into account the enhancement of the material properties.

The compression tests were performed on cold-formed stainless steel tubular X-joints fabricated with brace members fully welded at right angles to the opposing sides of the continuous chord members. The welded SHS and RHS consisted of a large range of section sizes. For the chord members, the tubular hollow sections had nominal overall flange width (b_0) ranged from 40 to 200

mm, nominal overall depth of the web (h_0) from 40 to 150 mm, and nominal thickness (t_0) from 3 to 6 mm. For the brace members, the nominal overall flange width (b_1) ranged from 40 to 150 mm, nominal overall depth of the web (h_1) from 40 to 150 mm, and nominal thickness (t_1) from 2 to 6 mm. The nominal wall thickness of both chord and brace members go beyond the limits of the current fatigue design guidelines, in which the nominal wall thickness of hollow sections should not be less than 4 mm. The length of the chord member (L_0) was chosen as $5h_0+h_1$ to ensure that the stresses at the brace and chord intersection region are not affected by the ends of the chord member. The length of the brace member (L_1) was chosen as $2.5h_1$ to avoid the overall buckling of brace members. The measured cross-section dimensions of the cold-formed stainless steel tubular X-joints are shown in Table 1, using the nomenclature defined in Fig. 3.

3.3. Specimen labeling

The specimens are labeled according to their joint configuration, stainless steel types and cross-section dimensions of chord and brace members. For example, the label 'XD-C140×3-B40×2' defines the following stainless steel tubular X-joint:

- The first letter 'X' indicates the X-joint specimens.
- The second letter 'D' indicates that the stainless steel type of the specimen, which is duplex stainless steel. If the letter is 'H', it refers to high strength austenitic (HAS) stainless steel. If the letter is 'N', it refers to normal strength austenitic stainless steel type AISI 304.
- The third letter 'C' refers to chord member and the following expression '140×3' indicates the cross-section dimensions of the chord member, which having nominal overall depth of the web (h_0) of 140 mm and wall thickness (t_0) of 3 mm. The overall flange width (b_0) is purposely not shown for simplification.
- The fourth letter 'B' refers to brace member and the following expression '40×2' indicates the cross-section dimensions of the brace member, which having nominal overall depth of the web (h_1) of 40 mm and wall thickness (t_1) of 2 mm. Once again, the overall flange width (b_1) is purposely not shown.

3.4. Hot spot strain (HSSN) measurement

To obtain the strain distribution along the brace and chord intersection region, two types of strip strain gauges TML FXV-1-17-002LE and TML FCV-1-17-005LE, which are specially

designed for stress concentration measurements of stainless steel structural members were used. The strain gauge TML FXV-1-17-002LE, which consists of five uniaxial strain gauges at a 12 mm backing enables five strain values to be measured at 2 mm interval simultaneously. The strain gauge TML FCV-1-17-005LE, which consists of ten biaxial strain gauges at a 12 mm backing enables ten strain values to be measured at 2 mm interval simultaneously. These two types of strip strain gauges were positioned at typical hot spot locations recommended by the CIDECT Design Guide No. 8 [1] to identify the nonlinear strain distribution along the brace and chord intersection region.

In the fabrication of cold-formed stainless steel tubular X-joints, the seam weld of brace members was positioned parallel to the cross-section of chord member. Hence, the strip strain gauges were also positioned at the center of brace and chord intersection edges to measure the corresponding HSSNs. The typical hot spot locations adopted in this study comprised nine fixed lines from *A* to *I*, as shown in Fig. 1. In order to evaluate the effects of welding fabrication on the SCFs at brace and chord intersection region, the strip strain gauges were placed to the weld toe as closer as possible. The first point of strain measurement was 2 mm away from the weld toe and the four other points of strain measurement were within the specified distance, which is out of the extrapolation region recommended in the current fatigue design guidelines. In addition to the strip strain gauges for the stress concentration measurements, commonly used single element strain gauges with a gauge length of 5 mm (TML FLA-5-17) specific to stainless steel were also attached at the mid-length of brace member to measure the nominal strain caused by applied loads, which were used for the prediction of SCFs. These strain gauges were located at the corners of the cross-section to exclude the possible effects of local buckling. The positions of all types of strain gauges for stress concentration measurements in the experimental investigation are illustrated in Fig. 4.

3.5. Test rig and procedure

A servo-controlled hydraulic testing machine was used to apply axial compression force to the stainless steel tubular X-joints. A special fixed-ended bearing was designed to simulate the pure axial compression test without any bending moment. Load control was used to drive the hydraulic actuator at a constant speed of 30 kN/min for all test specimens. The stainless steel tubular X-joints were subjected to the incremental static loading, which was predetermined to avoid any occurrence of plastic strains at the joint intersection area. During the tests, the hydraulic actuator was ramped to

the predetermined loads. The strain readings were recorded by pausing the applied loads for 1.5 mins near the predetermined loads. This allowed the stress relaxation associated with plastic straining to take place and also taking consideration of the time lag caused by the data acquisition system. The applied loads were then increased to the next load level and held in place for another 1.5 mins near the predetermined loads, while the strain readings were taken again. This test procedure was repeated until the final predetermined load level was reached, and then the test was continued using displacement control that allows the test to be continued in the post-ultimate range. Two photographs of the test setup of strain concentration measurements for stainless steel tubular X-joints are shown in Figs. 5 and 6 for the overall and close up views, respectively.

3.6. Comparison of experimental and calculated nominal strains

To determine the SNCFs of stainless steel tubular X-joints, the nominal strain in the brace member due to the applied load which causes the HSSN needs to be predicted. Since the nominal stress can be calculated from the applied load divided by the cross-sectional area of the brace member, the nominal strain can then be obtained from the nominal stress using the Hooke's Law. The calculated nominal strain was verified experimentally using four single element strain gauges mounted at the mid-length of brace member to measure the nominal strain. The locations of strain gauges were far away from the effects of end conditions and brace-chord welded junction to ensure the uniform strain measurements. The experimentally determined nominal strain was plotted against the calculated nominal strain, as illustrated in Figs. 7-11 for different stainless steel tubular X-joints under different applied load levels. It is shown from the comparison that good agreement between these two methods was achieved, confirming that the calculation method is applicable to nominal strain estimation for the SCF calculations of stainless steel tubular X-joints.

3.7. Determination of SCF

In the static tests for SCFs of stainless steel tubular X-joints, the strain components perpendicular to the weld toe as well as strain components parallel to the weld toe corresponding to the predetermined applied loads were all obtained from the strip strain gauges. It was found that the strain value for all test specimens generally increases as the distance between the strain gauge point and the weld toe decreases. The strain direction may also change from tension to compression as the applied load increases, and from compression to tension as the distance between the strain gauge

point and the weld toe increases. The strain distribution at typical hot spot locations follow the same trend for different applied load levels, showing that the strains were measured within the elastic response of stainless steel tubular X-joints, in this range high-cycle fatigue usually occurs. Furthermore, the maximum strains at brace and chord members under different applied load levels are generally within 10% of the strains corresponding to the 0.2% tensile proof stress of stainless steel tubes as shown in Tables 2 and 3, indicating that plastic strains generally do not occur at the brace and chord intersection region.

The HSSN $\xi_{\perp}$, which is perpendicular to the weld toe, and another strain component $\xi_{//}$, which is parallel to the weld toe were obtained by using the quadratic extrapolation method based on the recommendation given in the CIDECT Design Guide No. 8 [1] for SHS and RHS tubular joints. The SNCF which is easier to obtain from strain gauge measurement can be calculated as:

$$SNCF = \xi_{\perp} / \xi_n \tag{1}$$

where ξ_n is the nominal strain obtained from single element strain gauges which were placed at the mid-length of brace member. In order to obtain the SCF, the relationship between the SCF and SNCF needs to be determined. It was reported by Shao [15] that the relationship between SCF and SNCF can be expressed as:

$$SCF = \frac{1+\nu\dfrac{\varepsilon_{//}}{\varepsilon_{\perp}}}{1-\nu^2} SNCF \tag{2}$$

where ν is the Possion's ratio. In the static tests, the coefficient between SCF and SNCF can be determined by the ratio of strain component $\xi_{//}$ to HSSN $\xi_{\perp}$. The value of this coefficient ranged from 0.6 to 1.4. This coefficient was proposed by Dutta [16] to be equal to 1.2 for CHS tubular joints and 1.1 for SHS tubular joints, which was also recommended by the CIDECT Design Guide No. 8 [1] for CHS, SHS and RHS tubular joints based on the studies of Frater [17] and van Deflt et al. [18]. In this study, the coefficient between SCF and SNCF was investigated at typical hot spot locations as summarized in Tables 2 and 3 for stainless steel tubular X-joints of XD-C140×3-B140×3 and XH-C110×4-B150×6, respectively. It can be generally concluded from the tables that this coefficient is more or less constant at typical hot spot locations under different applied load levels. Thus, the coefficient between SCF and SNCF was obtained by averaging all the values at every hot spot locations under different applied load levels, excluding the abnormal

predictions resulted from deviation of strain gauge placement and sensitivity of the quadratic extrapolation method to relatively small extrapolation region for thin-walled tubular joints. In this study, an average value of this coefficient was calculated as 1.08 for stainless steel tubular X-joints. The SNCF can then be converted to SCF by using the expression of SCF = 1.08*SNCF for SHS and RHS stainless steel tubular X-joints.

The resulting SCFs obtained from the corresponding SNCFs at all hot spot locations were summarized in Table 4 for stainless steel tubular X-joints. The average values of SNCFs at typical hot spot locations were calculated by averaging all the values at every applied load levels, excluding the maximum and minimum values to eliminate the unstable strain measurements from small applied loads and any drift of strain measurements from comparatively large applied loads. Some conclusions can be drawn from the table as follows:

- The highest SCFs are usually found for stainless steel tubular X-joints with medium β values.
- The highest SCFs may occur at the center of brace and chord intersection edges as well as the traditional hot spot locations for stainless steel tubular X-joints.
- The SCFs at the brace and chord intersection region are not totally symmetric due to the existence of seam weld of brace members. The SCFs at hot spot locations near the seam weld of brace members are generally higher.
- The lower the 2γ ratio, the lower the SCF.
- It seems that the configuration of weld and the local condition of the weld toe have less influence on the stress concentrations of stainless steel tubular X-joints. The strain gauges can be positioned to the weld toe as close as possible.

4. Design guidelines

The SCFs of SHS and RHS carbon steel tubular X-joints under axial compression force can be determined using the following parametric equations given in the CIDECT Design Guide No. 8 [1]:

Chord member (hot spot locations *B*, *C* and *D*):

$$SCF_B = \left(0.143 - 0.204 \cdot \beta + 0.064 \cdot \beta^2\right) \cdot \left(2\gamma\right)^{\left(1.377 + 1.715 \cdot \beta - 1.103 \cdot \beta^2\right)} \cdot \tau^{0.75} \quad (3)$$

$$SCF_C = \left(0.077 - 0.129 \cdot \beta + 0.061 \cdot \beta^2 - 0.0003 \cdot 2\gamma\right) \cdot \left(2\gamma\right)^{\left(1.565 + 1.874 \cdot \beta - 1.028 \cdot \beta^2\right)} \cdot \tau^{0.75} \quad (4)$$

$$SCF_D = \left(0.208 - 0.387 \cdot \beta + 0.209 \cdot \beta^2\right) \cdot \left(2\gamma\right)^{\left(0.925 + 2.389 \cdot \beta - 1.881 \cdot \beta^2\right)} \cdot \tau^{0.75} \quad (5)$$

For tubular X-joints with β = 1.0:

SCF_C is multiplied by a factor of 0.65, SCF_D is multiplied by a factor of 0.50.

Brace member (hot spot locations *A* and *E*):

$$SCF_A = SCF_E = \left(0.013 + 0.693 \cdot \beta - 0.278 \cdot \beta^2\right) \cdot (2\gamma)^{\left(0.790 + 1.898 \cdot \beta - 2.109 \cdot \beta^2\right)} \quad (6)$$

For tubular joints with fillet welds:

Both SCF_A and SCF_E are multiplied by a factor of 1.40 for brace side of weld.

In which, the validity range of the parameters are: $0.35 \le \beta \le 1.0$; $12.5 \le 2\gamma \le 25$; $0.25 \le \tau \le 1.0$.

The experimental SCFs at typical hot spot locations (lines *A* to *E*) were compared with the SCFs calculated using the above parametric equations for stainless steel tubular X-joints, as shown in Table 4. The ratios of the maximum SCFs from the laboratory tests to the maximum SCFs from the design formulae given in the CIDECT are also summarized in Table 4, with values all less than 1.0 and as low as 0.18. It is shown from the comparison that the design formulae given in the CIDECT are quite unconservative for the prediction of the SCFs of stainless steel tubular X-joints, which is understood since the CIDECT design equations were derived from carbon steel instead of stainless steel. However, the hot spot locations where the highest SCFs occurred can be precisely captured by the fatigue design guideline. Hence, a new parametric equation for accurate prediction of the SCFs of stainless steel tubular X-joints is needed.

5. Finite element analysis

5.1. General

The FEM is another feasible way to determine the SCFs of welded tubular joints. The general purpose finite element program ABAQUS [19] was used in this study for the prediction of the SCFs of stainless steel tubular X-joints. The finite element analysis, which considers various influential factors, such as the modelling of weld profile, loading and boundary conditions are detailed in Feng and Young [20] for finite element modelling of cold-formed stainless steel tubular joints. However, all finite element analyses carried out in this study are linear elastic modelling to ensure that the SCFs at typical hot spot locations are not affected by different load levels within the elastic range. The material properties of stainless steel tubes given by Feng and Young [21] and welding material with the corresponding measured Young's modulus (E) and Poisson's ratio (ν = 0.3) were

incorporated in the finite element model.

5.2. Finite element type and mesh size

In the current finite element simulation, three-dimensional 20-noded solid element with an reduced integration scheme of 2×2×2 (C3D20R) was used to model the tubular sections as well as the weld profile, which was recommended by the CIDECT Design Guide No. 8 [1]. The round corners of SHS and RHS were also modelled with four-element mesh density based on the recommendation of Herion [22] to consider its influence on the SCFs. The convergence studies were carried out to obtain the optimum finite element mesh density. The weld area and the extrapolation region along the brace and chord interaction are fine meshed, whereas the mesh size at the location away from the interest area is gradually coarse in order to save computing cost. For thick-walled tubular members with ($b_0/t_0 \leq 20$ for chord member; and $b_1/t_1 \leq 20$ for brace member), four layers of solid elements were employed across the tube wall thickness, while for thin-walled tubular members with ($b_0/t_0 > 20$ for chord member; and $b_1/t_1 > 20$ for brace member), two layers of solid elements were used, as recommended by Choo et al. [23] and Feng and Young [20] for finite element modelling of welded tubular X-joints. The typical finite element modelling of stainless steel tubular X-joints for the prediction of all HSSNs and nominal strains are clearly shown in Fig. 12.

5.3. Loading and boundary conditions

The static compression force was applied in increments at each node of the loaded end by using the (*STATIC) method available in the ABAQUS library. The nodes other than the loaded and fixed ends were free to translate and rotate in any directions. Five consecutive load steps were required to complete the linear elastic finite element analysis, which was identical to the laboratory tests for each specimen. The HSSNs perpendicular to the weld toes at typical hot spot locations were obtained corresponding to the specific applied load levels. A quarter of tubular joint was modelled by making use of two planes of symmetry in geometry, loading application and boundary conditions. The nodal displacement perpendicular to the plane of symmetry is restrained while the two remaining transitional degrees of freedom are free.

5.4. Verification of finite element model

The SNCFs at typical hot spot locations obtained from the laboratory tests ($SNCF_{EXP}$) were compared with those predicted by the numerical analysis ($SNCF_{FE}$) in order to verify the finite element model for stainless steel tubular X-joints, as shown in Table 5. A minimum SCF of 2.0 is adopted for all hot spot locations based on the recommendation given in the CIDECT Design Guide No. 8 [1]. Therefore, relatively larger comparison difference for the SCFs less than 2.0 is considered to be acceptable. Generally, good agreement between the experimental and finite element analysis results was achieved. Therefore, the newly developed finite element model was verified with the test results and considered to be accurate and reliable.

6. Parametric study

6.1. Specimen description

By using the verified finite element model, an extensive parametric study was carried out to evaluate the effects of main parametric variations on the SCFs of cold-formed stainless steel tubular X-joints. A total of 115 X-joints in cold-formed stainless steel SHS and RHS tubes was analyzed in the parametric study. The similar label system as that defined in the experimental program based on the joint configuration and cross-section dimensions of chord and brace members was adopted. For example, the label 'XC400×240×8-B240×120×8' defines a tubular X-joint, indicated by the letter 'X'; the letter 'C' refers to chord member and the following expression '400×240×8' indicates the cross-section dimensions of chord member, which having overall depth of the web (h_0) of 400 mm, overall flange width (b_0) of 240 mm, and wall thickness (t_0) of 8 mm; the letter 'B' refers to brace member and the following expression '240×120×8' indicates the cross-section dimensions of brace member, which having overall depth of the web (h_1) of 240 mm, overall flange width (b_1) of 120 mm, and wall thickness (t_1) of 8 mm.

The welded SHS and RHS consisted of a large range of section sizes, which were selected within the range of practical applications. For the chord members, the tubular hollow sections have overall flange width (b_0) ranged from 30 to 300 mm, overall depth of the web (h_0) from 30 to 400 mm, and wall thickness (t_0) from 1 to 16 mm. For the brace members, the tubular hollow sections have overall flange width (b_1) ranged from 30 to 300 mm, overall depth of the web (h_1) from 30 to

400 mm, and wall thickness (t_1) from 1 to 16 mm. The wall thickness of both chord and brace members go beyond the limits of the current design guidelines, in which the wall thickness of hollow sections should not be less than 4 mm. The external corner radius (R_i) of stainless steel tube was taken as 2.5t when the thickness of tube (t) is larger than 3 mm, otherwise the external corner radius was taken to be 2t, which was recommended by the AISC design guideline [24]. The weld size (w) was taken as 2t based on the recommendation given in the American Welding Society (AWS) D1.1/D1.1M specification [25], where t is the thickness of thinner part between brace and chord members.

6.2. Influential parameters

The effects of main geometric parameters on the SCFs of cold-formed stainless steel tubular X-joints were evaluated separately, which include the brace to chord width ratio ($\beta = b_1/b_0$); the brace to chord thickness ratio ($\tau = t_1/t_0$) and the chord width to thickness ratio ($2\gamma = b_0/t_0$). The validity range of these parametric variations defined in the CIDECT Design Guide No. 8 [1] for carbon steel tubular structures and those applied in the laboratory tests as well as designed for the parametric study are summarized in Table 6. It is shown from the table that the parametric variations designed in the parametric study are significantly beyond the validity range of those defined in the current design guideline for welded tubular X-joints. Furthermore, the thickness of the tubes is as low as 1 mm, which is well beyond the current limit of not less than 4 mm.

The parametric study was performed by evaluating the effect of one particular parametric variation at a time while the others were maintained constant. The material properties of duplex stainless steel tube 140×80×3 given by Feng and Young [21] and welding material with the corresponding measured Young's modulus (E) and Poisson's ratio (v = 0.3) were used in the parametric study. The static uniform loads were initially applied by means of displacement to obtain the full load-deformation curves. The compression forces were then applied by the consecutive load steps as load control within the predetermined elastic range to avoid any occurrence of plastic strains at the joint intersection region. The main parametric variations designed in the parametric study and the SCFs at typical hot spot locations determined from the finite element analysis are summarized in Table 7.

6.3. Numerical analysis

The HSSs at the hot spot locations *A*, *E*, *F* and *H* were compared with each other since they are defined along the same direction at the brace member. It is shown from the comparison that the SCFs at line *A* are always larger than the SCFs at lines *E* and *F* and generally larger than the SCFs at line *H*. Therefore, the proposed design equation to predict the maximum SCFs of the brace member is based on lines *A* and *H* only instead of deriving different design formulae for lines *A*, *E*, *F* and *H*, respectively. The similar approach was established to estimate the maximum SCFs of the chord member. It is shown from Table 7 that the SCFs at line *B* are always larger than the SCFs at line *I*; the SCFs at line *D* are always larger than the SCFs at line *G*, except for specimen XC40×40×4-B40×40×4. The SCFs for this specimen at lines *B* and *D* are a little bit smaller than the SCFs at the lines *I* and *G*, respectively. The difference is quite small and the SCFs at all hot spot locations are below the value of 2.0. Hence, the proposed design equation is based on lines *B*, *C* and *D* only to determine the maximum SCFs of the chord member.

6.4. Comparison of SCFs obtained from parametric study and current design formulae

The SCFs obtained from the parametric study were compared with the SCFs calculated using the design formulae given in the CIDECT Design Guide No. 8 [1]. It should be noted that the design formulae given in this guideline are only applicable to the SCFs at hot spot locations *A*, *B*, *C*, *D* and *E*. Therefore, the SCFs at hot spot locations *F*, *G*, *H* and *I* were not taken into consideration. The comparison of the SCFs at hot spot locations *A*, *B*, *C* and *D* for all specimens is shown in Table 8. The mean values of FE SCF-to-CIDECT SCF ratio (SCF_{FE}/SCF_{CIDECT}) are 0.80, 0.99, 0.17 and 0.54, with the corresponding coefficients of variation (COV) of 0.350, 1.069, 3.071 and 0.932 for hot spot locations *A*, *B*, *C* and *D*, respectively. It can be generally concluded from the comparison that the design formulae specified in the current design guideline are quite unconservative for stainless steel tubular X-joints at hot spot locations *A*, *C* and *D*. It is appropriate for hot spot location *B*, but the degree of scatter is quite large.

7. Proposed design equation for SCFs at typical hot spot locations

Based on the study of van Wingerde [26] and design formulae given in the CIDECT Design Guide No. 8 [1] for carbon steel tubular X-joints, the unified design equation for the SCFs of

stainless steel SHS and RHS tubular X-joints subjected to axial compression force is proposed as follows:

$$SCF = \left(a + b \cdot \beta + c \cdot \beta^2 + d \cdot 2\gamma\right) \cdot \left(2\gamma\right)^{\left(e + f \cdot \beta + g \cdot \beta^2\right)} \cdot \tau^h \quad (7)$$

where the constants *a*, *b*, *c*, *d*, *e*, *f*, *g* and *h* change for typical hot spot locations *A* to *I*. These coefficients were determined by the least squares method, as summarized in Table 9. It was found that these coefficients can be rounded off to three decimal places without compromising the accuracy, except for the coefficient *d*, which should be rounded off to four decimal places.

The SCFs obtained from the parametric study are compared with the SCFs calculated using the proposed unified design equation for stainless steel SHS and RHS tubular X-joints. The comparison for all specimens is shown in Table 8 for the SCFs at hot spot locations *A*, *B*, *C*, *D* and *H*, respectively. A good agreement was obtained with the mean values of FE SCF-to-Proposed SCF ratio ($SCF_{FE}/SCF_{Proposed}$) of 1.00, 1.00, 1.00, 1.00 and 1.00, and the corresponding COV of 0.281, 0.177, 0.316, 0.279 and 0.211.

8. Conclusions

Experimental and numerical investigations on the SCFs of cold-formed stainless steel SHS and RHS tubular X-joints were conducted in this study. Both high strength stainless steel (duplex and high strength austenitic) and normal strength stainless steel (AISI 304) tubular X-joints were investigated. The newly developed finite element model was verified against the experimental results. An extensive parametric study was performed by using the verified finite element model to evaluate the effects of the main geometric parameters (β, τ and 2γ) on the SCFs of cold-formed stainless steel tubular X-joints at typical hot spot locations. The results of the parametric study were compared with the CIDECT design predictions for SHS and RHS tubular X-joints. It is shown from the comparison that the design rules specified in the current design guideline are generally quite unconservative for the SCFs of cold-formed stainless steel tubular X-joints. The values obtained from the proposed unified design equation for the SCFs of cold-formed stainless steel tubular X-joints are generally much more accurate than those calculated using the current design formulae. The limit of the geometric parameters (β, τ and 2γ) and the thickness of the tubular sections in the proposed unified design equation are beyond the limit in the CIDECT design formulae.

Acknowledgements

The authors are grateful to STALA Tube Finland for supplying the test specimens. The authors are also thankful to Mr. Yuet-Wang Kam for his assistance in the experimental program as part of his final year undergraduate research project at The University of Hong Kong.

References

[1] Zhao XL, Herion S, Packer JA, Puthli RS, Sedlacek G, Wardenier J, Weynand K, van Wingerde AM, Yeomans NF. Design guide for circular and rectangular hollow section welded joints under fatigue loading. Comité International pour le Développement et l'Étude de la Construction Tubulaire (CIDECT), Verlag TÜV Rheinland, Berlin, Germany, 2001.

[2] Toprac AA, Natarajan M, Erzurumlu H, Kanoo ALJ. Research in tubular joints: Static and fatigue loads. Offshore Technological Conference, OTC 1062, Houston, USA, 1969. p. 667-680.

[3] Kuang JG, Potvin AB, Leick RD. Stress concentration in tubular joints. Offshore Technological Conference, OTC 2205, Houston, USA, 1975. p. 593-612.

[4] Gibstein MB. Parametric stress analysis of T joints. European Offshore Steels Research Seminar, Cambridge, UK, 1978. p. 9P26.1-9P26.15.

[5] Romeijn A, Puthli RS, Wardenier J. Guidelines on the numerical determination of stress concentration factors of tubular joints. Proceedings of the Fifth International Symposium on Tubular Structures, Nottingham, UK, 1993. p. 625-639.

[6] Macdonald KA, Haagensen PJ. Fatigue design of welded aluminum rectangular hollow section joints. Engineering Failure Analysis 1999; 6(2): 113-130.

[7] van Wingerde AM, Packer JA, Wardenier J. Criteria for the fatigue assessment of hollow structural section connections. Journal of Constructional Steel Research 1995; 35(1): 71-115.

[8] International Institute of Welding (IIW). Recommended fatigue design procedure for hollow section joints. Part 1-hot spot stress method for nodal joints. IIW Subcommission XV-E, IIW Doc. XV-582-85, IIW Assembly, Strasbourg, France, 1985.

[9] Department of Energy (DEn). Offshore installation: Guidance on design and construction. Department of Energy, London, UK, 1990.

[10] Eurocode 3 (EC3). Design of steel structures-Part 1-9: Fatigue. European Committee for Standardization, EN 1993-1-9, CEN, Brussels, Belgium, 2005.

[11] American Welding Society (AWS). Structural welding code-steel, ANSI-AWS D1.1-98, Miami, USA, 1998.

[12] American Petroleum Institute (API). Recommended practice for planning, designing and

constructing fixed offshore platforms, API-PR2A, Dallas, USA, 1991.

[13] Radenkovic D. Stress analysis in tubular joints. Steel in Marine Structures, Paris, France, 1981. p. 53-95.

[14] Gibstein MB, Moe ET. Fatigue of tubular joints. In: Almar-Naess T, editor. Fatigue handbook, 1985.

[15] Shao YB. Fatigue behaviour of uniplanar tubular K-joints under axial and in-plane bending loads. PhD thesis, Nanyang Technological University, Singapore, 2004.

[16] Dutta D. Parameters influencing the stress concentration factors in joints in offshore structures. Fatigue in offshore structures, Rotterdam, The Netherlands, 1996. p. 77-128.

[17] Frater GS. Performance of welded rectangular hollow structural section trusses. PhD thesis, University of Toronto, Canada, 1991.

[18] van Deflt DRV, Noordhoek C, Da Re ML. The results of the European fatigue tests on welded tubular joints compared with SCF formulas and design lines. Steel in Marine Structures, Delft, The Netherlands, 1987. p. 565-577.

[19] Hibbitt, Karlsson and Sorensen, Inc. ABAQUS standard user's manual, vols. 1-3, version 6.7. USA, 2007.

[20] Feng R, Young B. Design of cold-formed stainless steel tubular T- and X-joints. Journal of Constructional Steel Research 2011; 67(3): 421-436.

[21] Feng R, Young B. Tests and behaviour of cold-formed stainless steel tubular X-joints. Thin-Walled Structures 2010; 48(12): 921-934.

[22] Herion S. Multiplanar K-joints made of RHS. PhD thesis, University of Karlsruhe, Germany, 1994.

[23] Choo YS, Qian XD, Liew JYR, Wardenier J. Static strength of thick-walled CHS X-joints-Part I. New approach in strength definition. Journal of Constructional Steel Research 2003; 59(10): 1201-1228.

[24] Australian Institute of Steel Construction (AISC). Design capacity tables for structural steel hollow sections. Sydney, Australia, 1992.

[25] American Welding Society (AWS). Structural welding code-steel. AWS D1.1/1.1M, Miami, USA, 2004.

[26] van Wingerde AM. The fatigue behaviour of T- and X-joints made of square hollow sections. PhD thesis, Delft University of Technology, The Netherlands, 1992.

Notation

a,b,c,d,e,f,g,h	Coefficients for proposed design equations
b_0	Overall width of chord member
b_1	Overall width of brace member
COV	Coefficient of variation
E	Young's modulus of elasticity obtained from longitudinal tensile coupon test
h_0	Overall depth of chord member
h_1	Overall depth of brace member
L_0	Overall length of chord member
L_1	Overall length of brace member
r	Corner radius of tubular member
r_0	Inner corner radius of chord member
r_1	Inner corner radius of brace member
R_i	External corner radius of stainless steel tube
SCF_A,SCF_B,SCF_C SCF_D,SCF_E	Stress concentration factors at typical hot spot locations
SCF_{CIDECT}	Stress concentration factor obtained from CIDECT rules
SCF_{EXP}	Stress concentration factor obtained from experimental investigation
SCF_{FE}	Stress concentration factor obtained from finite element analysis
$SCF_{Proposed}$	Stress concentration factor obtained from proposed design equations
$SNCF_{EXP}$	Strain concentration factor obtained from experimental investigation
$SNCF_{FE}$	Strain concentration factor obtained from finite element analysis
S/N	SCF to SNCF ratio ($SCF/SNCF$)
t	Overall thickness of tubular member
t_0	Overall thickness of chord member
t_1	Overall thickness of brace member
w	Weld size
w'	Weld size for full width joint
β	Brace to chord width ratio (b_1/b_0)
2γ	Chord width to thickness ratio (b_0/t_0)

ε_{Bmax}	Maximum strain at brace member
$\varepsilon_{B0.2}$	Strain corresponding to 0.2% tensile proof stress of brace member
ε_{Cmax}	Maximum strain at chord member
$\varepsilon_{C0.2}$	Strain corresponding to 0.2% tensile proof stress of chord member
ν	Poisson's ratio
ξ_n	Nominal strain
$\xi_{\perp}$	Hot spot strain perpendicular to weld toe
$\xi_{//}$	Strain parallel to weld toe
τ	Brace to chord thickness ratio (t_1/t_0)

Specimen	Chord (mm)					Brace (mm)					Weld (mm)		
	h_0	b_0	t_0	r_0	L_0	h_1	b_1	t_1	r_1	L_1	w	w'	β
XD-C140×3-B40×2	140.2	80.2	3.33	6.5	737	39.9	40.3	1.96	2.0	99	6.6	—	0.50
XD-C140×3-B140×3	140.0	80.1	3.09	6.5	851	140.1	80.1	3.10	6.5	346	6.6	8.5	1.00
XH-C150×6-B150×6	150.3	150.5	5.75	6.0	902	150.3	150.3	5.84	6.0	368	9.2	15.5	1.00
XH-C110×4-B150×6	110.3	196.3	3.98	8.5	698	150.3	150.4	5.82	6.0	365	9.6	—	0.77
XN-C40×4-B40×2	40.1	40.0	3.79	4.0	240	40.2	40.1	1.97	2.0	98	6.5	11.9	1.00

Table 1. Measured specimen dimensions of stainless steel tubular X-joints

Hot spot location	Axial compression force (kN)															Average S/N ratio
	19.9			40.1			59.8			80.3			99.5			
	$\varepsilon_{Bmax}/\varepsilon_{B0.2}$ = 1.1%			$\varepsilon_{Bmax}/\varepsilon_{B0.2}$ = 3.5%			$\varepsilon_{Bmax}/\varepsilon_{B0.2}$ = 5.8%			$\varepsilon_{Bmax}/\varepsilon_{B0.2}$ = 8.2%			$\varepsilon_{Bmax}/\varepsilon_{B0.2}$ = 10.9%			
	$\varepsilon_{Cmax}/\varepsilon_{C0.2}$ = 1.4%			$\varepsilon_{Cmax}/\varepsilon_{C0.2}$ = 1.9%			$\varepsilon_{Cmax}/\varepsilon_{C0.2}$ = 2.6%			$\varepsilon_{Cmax}/\varepsilon_{C0.2}$ = 3.2%			$\varepsilon_{Cmax}/\varepsilon_{C0.2}$ = 3.9%			
	$\xi_{\perp}$	$\xi_{//}$	S/N	$\xi_{\perp}$	$\xi_{//}$	S/N	$\xi_{\perp}$	$\xi_{//}$	S/N	$\xi_{\perp}$	$\xi_{//}$	S/N	$\xi_{\perp}$	$\xi_{//}$	S/N	
A	-40.2	26.6	0.88	-121.6	53.4	0.95	-204.0	80.4	0.97	-295.6	113.6	0.97	-388.6	148.4	0.97	0.948
B	20.1	44.0	1.82	-20.5	83.2	-0.24	-76.6	112.6	0.61	-155.0	139.2	0.80	-245.9	167.0	0.87	1.025
C	41.4	37.6	1.40	51.8	67.6	1.53	59.2	92.2	1.61	60.8	105.8	1.67	67.8	121.0	1.69	1.580
D	58.4	12.0	1.17	77.6	-20.4	1.01	95.8	-61.0	0.89	105.6	-108.8	0.76	115.2	-164.0	0.63	0.892
E	-46.2	17.3	0.98	-150.8	22.7	1.05	-247.4	25.1	1.07	-353.6	34.3	1.07	-465.4	38.5	1.07	1.048
Average S/N ratio for all hot spot locations																**1.10**

Table 2. SCF/SNCF ratios for stainless steel tubular X-joint of specimen XD-C140×3-B140×3 (β=1.00, τ=1.00, 2γ=25.92)

Hot spot location	Axial compression force (kN)															Average S/N ratio
	16.1			32.1			47.9			64.0			79.8			
	$\varepsilon_{Bmax}/\varepsilon_{B0.2}$ = 3.5%			$\varepsilon_{Bmax}/\varepsilon_{B0.2}$ = 6.3%			$\varepsilon_{Bmax}/\varepsilon_{B0.2}$ = 8.0%			$\varepsilon_{Bmax}/\varepsilon_{B0.2}$ = 9.2%			$\varepsilon_{Bmax}/\varepsilon_{B0.2}$ = 10.0%			
	$\varepsilon_{Cmax}/\varepsilon_{C0.2}$ = 1.5%			$\varepsilon_{Cmax}/\varepsilon_{C0.2}$ = 3.8%			$\varepsilon_{Cmax}/\varepsilon_{C0.2}$ = 6.5%			$\varepsilon_{Cmax}/\varepsilon_{C0.2}$ = 9.8%			$\varepsilon_{Cmax}/\varepsilon_{C0.2}$ = 13.6%			
	$\xi_{\perp}$	$\xi_{//}$	S/N	$\xi_{\perp}$	$\xi_{//}$	S/N	$\xi_{\perp}$	$\xi_{//}$	S/N	$\xi_{\perp}$	$\xi_{//}$	S/N	$\xi_{\perp}$	$\xi_{//}$	S/N	
A	-160.4	26.4	1.04	-289.4	59.8	1.03	-366.8	102.8	1.01	-418.0	154.8	0.98	-456.0	213.6	0.94	1.000
B	-324.6	-18.0	1.12	-709.0	-36.2	1.12	-1100.2	-49.0	1.11	-1476.6	-71.0	1.11	-1848.6	-101.6	1.12	1.116
C	-207.8	-87.0	1.24	-494.2	-202.8	1.23	-809.2	-336.0	1.24	-1136.6	-476.6	1.24	-1496.6	-646.2	1.24	1.238
D	-65.6	-79.8	1.50	-172.6	-187.4	1.46	-295.4	-307.6	1.44	-441.0	-437.6	1.43	-615.0	-593.6	1.42	1.450
E	-4.4	23.8	-0.68	-24.0	60.2	0.27	-55.4	108.6	0.45	-99.8	162.6	0.56	-153.4	228.4	0.61	0.473
Average S/N ratio for all hot spot locations																**1.06**

Table 3. SCF/SNCF ratios for stainless steel tubular X-joint of specimen XH-C110×4-B150×6 (β=0.77, τ=1.46, 2γ=49.32)

Specimen	$\beta=b_1/b_0$	$\tau=t_1/t_0$	$2\gamma=b_0/t_0$	Comparison	Stress concentration factor (SCF)				
					A	B	C	D	E
XD-C140×3-B40×2	0.50	0.59	24.08	Experiment	2.19	***16.23***	10.28	4.74	1.37
				CIDECT	19.21	***19.46***	17.42	8.50	19.21
				SCF_{EXP}/SCF_{CIDECT}	0.11	***0.83***	0.59	0.56	0.07
XD-C140×3-B140×3	1.00	1.00	25.92	Experiment	***2.49***	0.15	0.73	-0.55	1.39
				CIDECT	***3.95***	1.95	2.04	1.60	3.95
				SCF_{EXP}/SCF_{CIDECT}	***0.63***	0.08	0.36	-0.34	0.35
XH-C150×6-B150×6	1.00	1.02	26.17	Experiment	***2.28***	2.06	0.98	-0.11	1.64
				CIDECT	***4.01***	2.08	2.00	1.64	4.01
				SCF_{EXP}/SCF_{CIDECT}	***0.57***	0.99	0.49	-0.07	0.41
XH-C110×4-B150×6	0.77	1.46	49.32	Experiment	5.62	***16.51***	12.14	4.47	0.84
				CIDECT	26.93	***93.02***	-12.55	28.38	26.93
				SCF_{EXP}/SCF_{CIDECT}	0.21	***0.18***	-0.97	0.16	0.03
XN-C40×4-B40×2	1.00	0.52	10.55	Experiment	***1.16***	0.56	0.09	-0.04	0.81
				CIDECT	***2.31***	0.19	0.68	0.27	2.31
				SCF_{EXP}/SCF_{CIDECT}	***0.50***	2.95	0.13	-0.15	0.35

Table 4. Comparison of experimental SCFs with values calculated using design formulae given in the CIDECT

Specimen	Comparison	Strain concentration factor (SNCF)								
		A	B	C	D	E	F	G	H	I
XD-C140×3-B40×2	Experiment	—	15.03	9.52	4.39	1.27	-0.79	—	4.26	12.27
	FE model	—	15.38	8.82	3.74	0.86	-1.33	—	4.26	9.04
	$SNCF_{EXP}/SNCF_{FE}$	—	0.98	1.08	1.17	1.48	0.59	—	1.00	1.36
XH-C150×6-B150×6	Experiment	2.11	1.91	0.91	—	1.52	0.35	0.09	2.49	1.69
	FE model	2.27	2.13	1.01	—	2.16	0.27	0.06	1.55	1.37
	$SNCF_{EXP}/SNCF_{FE}$	0.93	0.90	0.90	—	0.70	1.30	1.50	1.61	1.23
XN-C40×4-B40×2	Experiment	1.07	0.52	0.08	-0.04	0.75	1.19	0.04	1.63	0.72
	FE model	1.19	0.67	0.16	-0.03	1.20	0.74	0.04	1.14	0.65
	$SNCF_{EXP}/SNCF_{FE}$	0.90	0.78	0.50	1.33	0.63	1.61	1.00	1.43	1.11

Table 5. Comparison of experimental SNCFs with values obtained from finite element analysis

Geometric parameter	$\beta=b_1/b_0$	$\tau=t_1/t_0$	$2\gamma=b_0/t_0$
CIDECT	[0.35-1.0]	[0.25-1.0]	[12.5-25.0]
Laboratory tests	[0.5-1.0]	[0.5-1.5]	[10.0-50.0]
Parametric study	[0.2-1.0]	[0.25-2.0]	[10.0-50.0]

Table 6. Validity range of geometric parameters

Specimen	β	τ	2γ	Stress concentration factor (SCF_{FE})								
				A	B	C	D	E	F	G	H	I
XC120×200×4-B30×40×1	0.2	0.25	50	9.27	12.17	12.30	7.34	6.88	-2.64	2.25	1.81	7.57
XC120×200×4-B50×40×1	0.2	0.25	50	12.90	15.27	15.30	9.12	9.34	-3.13	2.29	1.44	6.87
XC200×200×4-B30×40×1	0.2	0.25	50	9.60	12.75	12.74	7.39	6.96	-2.88	2.16	2.01	7.99
XC200×200×4-B50×40×1	0.2	0.25	50	13.46	16.11	15.97	9.24	9.53	-3.48	2.16	1.56	7.33
XC60×60×2-B30×30×1	0.5	0.50	30	6.77	17.67	13.65	6.53	2.01	-0.28	0.49	6.76	9.08
XC60×60×2-B50×30×1	0.5	0.50	30	7.89	20.21	15.60	7.47	2.45	0.14	0.22	5.64	6.58
XC100×60×2-B30×30×1	0.5	0.50	30	7.01	18.52	14.23	6.47	1.91	-0.48	0.29	7.02	9.61
XC100×60×2-B50×30×1	0.5	0.50	30	8.25	21.44	16.45	7.48	2.37	-0.08	-0.04	5.86	7.11
XC60×100×2-B30×50×1	0.5	0.50	50	10.86	29.69	27.33	12.88	3.65	1.39	0.96	9.93	18.01
XC60×100×2-B50×50×1	0.5	0.50	50	13.59	36.41	33.43	15.97	4.75	2.94	-0.58	10.62	15.27
XC100×100×2-B30×50×1	0.5	0.50	50	11.38	31.46	28.62	12.84	3.49	1.20	0.64	10.44	19.27
XC100×100×2-B50×50×1	0.5	0.50	50	14.43	39.07	35.49	16.19	4.64	2.82	-1.09	11.20	16.65
XC30×50×1-B30×40×1	0.8	1.00	50	7.29	22.11	19.56	9.06	-0.43	0.58	0.21	10.45	9.61
XC30×50×1-B50×40×1	0.8	1.00	50	8.06	24.92	22.30	10.62	-0.41	1.40	-0.09	7.77	3.74
XC50×50×1-B30×40×1	0.8	1.00	50	7.51	24.01	21.04	8.93	-0.58	0.45	-0.08	10.69	10.95
XC50×50×1-B50×40×1	0.8	1.00	50	8.39	27.30	24.19	10.55	-0.56	1.30	-0.42	7.96	5.64
XC40×40×4-B30×40×1	1.0	0.25	10	1.40	0.28	0.01	0.17	0.99	0.56	0.16	1.22	0.26
XC40×40×4-B50×40×1	1.0	0.25	10	1.35	0.31	0.02	0.22	1.06	0.63	0.21	1.06	0.30
XC30×30×1-B30×30×1	1.0	1.00	30	2.12	1.78	0.28	-0.55	1.37	0.27	0.04	1.62	1.45
XC30×30×1-B50×30×1	1.0	1.00	30	2.00	1.65	0.25	-0.51	1.32	0.26	0.05	1.33	1.24
XC50×30×1-B30×30×1	1.0	1.00	30	2.17	1.94	0.80	-0.49	1.41	0.28	0.05	1.56	1.44
XC50×30×1-B50×30×1	1.0	1.00	30	2.08	1.81	0.58	-0.50	1.39	0.27	0.04	1.29	1.24
XC30×50×1-B30×50×1	1.0	1.00	50	2.67	2.61	0.31	-0.71	1.73	0.22	0.05	2.00	1.77
XC30×50×1-B50×50×1	1.0	1.00	50	2.57	2.10	0.26	-0.68	1.70	0.21	0.08	1.62	1.46
XC50×50×1-B30×50×1	1.0	1.00	50	2.74	2.43	0.91	-0.65	1.78	0.22	0.04	1.92	1.75
XC50×50×1-B50×50×1	1.0	1.00	50	2.69	2.31	0.59	-0.67	1.79	0.22	0.04	1.58	1.47
XC120×200×4-B40×40×4	0.2	1.00	50	9.07	42.74	30.95	19.05	0.54	-1.94	14.53	6.29	36.47
XC200×200×4-B40×40×4	0.2	1.00	50	9.60	45.14	32.15	18.85	0.17	-2.35	14.22	6.72	38.59
XC160×160×16-B40×80×4	0.5	0.25	10	3.84	1.20	1.71	1.13	1.95	0.32	0.43	3.34	1.02
XC160×160×16-B120×80×4	0.5	0.25	10	4.48	1.46	2.11	1.32	2.72	0.40	0.42	1.67	0.67
XC80×80×8-B40×40×4	0.5	0.50	10	3.40	1.84	2.25	1.19	1.00	0.44	0.96	2.97	1.41
XC240×240×8-B120×120×4	0.5	0.50	30	20.06	22.73	17.96	9.09	7.94	-0.08	0.42	6.67	9.96
XC240×240×8-B200×120×4	0.5	0.50	30	22.92	25.71	20.83	10.64	9.70	0.39	0.08	5.62	7.37
XC400×240×8-B120×120×4	0.5	0.50	30	20.77	23.77	18.65	9.03	7.78	-0.26	0.18	6.93	10.55
XC400×240×8-B200×120×4	0.5	0.50	30	23.97	27.21	21.89	10.67	9.61	0.18	-0.23	5.84	7.97
XC120×120×4-B40×60×4	0.5	1.00	30	10.65	30.82	15.99	6.76	-0.17	-1.86	3.02	8.49	26.63
XC120×120×4-B120×60×4	0.5	1.00	30	14.98	35.02	20.19	9.50	0.06	-1.89	4.50	8.61	13.94
XC200×120×4-B40×60×4	0.5	1.00	30	10.99	32.02	16.47	6.45	-0.42	-2.07	2.72	8.80	27.69
XC200×120×4-B120×60×4	0.5	1.00	30	15.58	37.04	21.11	9.23	-0.29	-2.19	4.17	8.92	14.99
XC120×200×4-B120×100×4	0.5	1.00	50	28.38	68.05	46.41	22.14	3.66	0.40	4.78	16.83	34.43
XC120×200×4-B200×100×4	0.5	1.00	50	32.71	77.26	52.82	25.59	4.22	1.67	5.53	16.71	26.31
XC200×200×4-B120×100×4	0.5	1.00	50	30.05	72.92	48.96	21.82	3.00	-0.04	4.09	17.76	37.24
XC200×200×4-B200×100×4	0.5	1.00	50	35.00	83.73	56.43	25.61	3.60	1.26	4.84	17.63	28.89

XC60×100×2-B40×50×4	0.5	2.00	50	16.20	111.19	62.76	25.03	-2.03	-2.60	10.38	12.96	98.12
XC100×100×2-B40×50×4	0.5	2.00	50	17.10	118.35	65.38	23.73	-2.67	-3.11	8.82	13.72	104.59
XC120×200×4-B120×160×4	0.8	1.00	50	23.67	33.09	19.60	8.73	1.84	0.60	0.41	10.41	11.42
XC120×200×4-B200×160×4	0.8	1.00	50	26.56	37.03	22.09	10.07	2.32	1.45	0.16	7.87	5.66
XC200×200×4-B120×160×4	0.8	1.00	50	24.44	35.04	20.14	8.50	1.50	0.46	0.16	10.65	12.40
XC200×200×4-B200×160×4	0.8	1.00	50	27.75	39.64	22.92	9.94	2.01	1.34	-0.13	8.07	6.97
XC60×100×2-B40×80×4	0.8	2.00	50	14.19	40.28	21.90	6.61	-1.88	-0.57	0.97	12.57	38.42
XC60×100×2-B120×80×4	0.8	2.00	50	16.25	41.08	24.83	8.73	-2.11	-0.31	1.63	10.71	19.09
XC100×100×2-B40×80×4	0.8	2.00	50	14.47	42.27	22.97	6.10	-2.14	-0.68	0.56	12.83	40.15
XC100×100×2-B120×80×4	0.8	2.00	50	16.83	44.56	26.69	8.21	-2.38	-0.43	1.17	10.88	22.28
XC160×160×16-B120×160×4	1.0	0.25	10	1.43	0.35	-0.01	0.33	1.12	0.57	0.12	1.23	0.29
XC160×160×16-B200×160×4	1.0	0.25	10	1.34	0.38	0.04	0.37	1.17	0.63	0.16	1.06	0.32
XC80×80×8-B40×80×4	1.0	0.50	10	1.56	0.76	0.28	0.29	1.11	0.67	0.05	1.54	0.73
XC80×80×8-B120×80×4	1.0	0.50	10	1.31	0.76	0.24	0.36	1.18	0.77	0.15	1.07	0.66
XC40×40×4-B40×40×4	1.0	1.00	10	1.44	1.22	0.33	0.18	1.10	0.99	0.23	1.46	1.23
XC120×120×4-B120×120×4	1.0	1.00	30	2.33	2.25	0.31	0.89	1.81	0.30	0.03	1.63	1.43
XC120×120×4-B200×120×4	1.0	1.00	30	2.16	2.05	0.28	0.83	1.71	0.27	0.04	1.32	1.20
XC200×120×4-B120×120×4	1.0	1.00	30	2.40	2.41	0.76	1.12	1.98	0.30	0.02	1.58	1.44
XC200×120×4-B200×120×4	1.0	1.00	30	2.27	2.22	0.56	1.02	1.88	0.29	0.02	1.29	1.22
XC120×200×4-B120×200×4	1.0	1.00	50	3.06	2.89	0.38	1.18	2.34	0.24	0.06	2.08	1.79
XC120×200×4-B200×200×4	1.0	1.00	50	2.82	2.62	0.31	1.11	2.17	0.23	0.08	1.62	1.41
XC200×200×4-B120×200×4	1.0	1.00	50	3.14	3.12	0.91	1.48	2.54	0.24	0.03	2.02	1.81
XC200×200×4-B200×200×4	1.0	1.00	50	2.95	2.85	0.60	1.33	2.39	0.23	0.03	1.59	1.46
XC60×60×2-B40×60×4	1.0	2.00	30	3.72	4.35	1.20	0.95	0.86	0.12	0.24	3.24	3.93
XC60×60×2-B120×60×4	1.0	2.00	30	3.26	3.63	1.19	0.81	0.86	0.17	0.31	2.55	1.79
XC100×60×2-B40×60×4	1.0	2.00	30	3.68	4.51	1.46	1.24	0.87	0.12	0.25	3.14	4.01
XC100×60×2-B120×60×4	1.0	2.00	30	3.47	4.05	1.23	0.97	0.96	0.17	0.27	2.45	1.91
XC60×100×2-B120×100×4	1.0	2.00	50	4.11	4.58	1.49	1.06	1.09	0.26	0.26	3.06	2.14
XC60×100×2-B200×100×4	1.0	2.00	50	3.83	4.28	1.41	1.04	1.06	0.28	0.30	2.58	1.48
XC100×100×2-B120×100×4	1.0	2.00	50	4.36	5.11	1.54	1.24	1.22	0.24	0.18	2.95	2.30
XC100×100×2-B200×100×4	1.0	2.00	50	4.05	4.77	1.48	1.17	1.17	0.27	0.23	2.66	1.80
XC160×160×16-B80×80×8	0.5	0.50	10	4.98	1.84	1.72	1.73	1.66	0.72	1.29	3.91	1.44
XC240×240×8-B80×120×8	0.5	1.00	30	15.47	34.64	19.33	7.60	0.72	-2.19	3.30	11.13	29.83
XC240×240×8-B240×120×8	0.5	1.00	30	21.29	39.42	24.75	10.69	1.58	-2.10	4.88	10.82	15.69
XC400×240×8-B80×120×8	0.5	1.00	30	15.95	35.97	19.88	7.25	0.39	-2.46	2.96	11.52	31.01
XC400×240×8-B240×120×8	0.5	1.00	30	22.13	41.68	25.86	10.39	1.12	-2.48	4.50	11.23	16.86
XC120×200×4-B80×100×8	0.5	2.00	50	25.13	124.92	68.01	26.19	-1.43	-2.95	10.76	17.54	103.80
XC200×200×4-B80×100×8	0.5	2.00	50	26.55	133.14	70.79	24.58	-2.32	-3.61	9.09	18.59	110.83
XC120×200×4-B80×160×8	0.8	2.00	50	20.13	53.18	19.54	5.95	-1.79	-0.65	0.94	15.61	42.95
XC120×200×4-B240×160×8	0.8	2.00	50	24.01	57.80	24.01	8.42	-1.99	-0.28	1.62	13.44	23.04
XC200×200×4-B80×160×8	0.8	2.00	50	20.55	55.09	19.81	5.32	-2.13	-0.79	0.51	15.94	44.43
XC200×200×4-B240×160×8	0.8	2.00	50	24.92	61.47	24.65	7.75	-2.37	-0.43	1.12	13.64	25.32
XC160×160×16-B80×160×8	1.0	0.50	10	1.54	0.81	0.27	0.46	1.22	0.73	0.04	1.52	0.75
XC160×160×16-B240×160×8	1.0	0.50	10	1.31	0.85	0.24	0.54	1.30	0.84	0.15	1.07	0.68
XC80×80×8-B80×80×8	1.0	1.00	10	1.46	1.29	0.33	0.48	1.26	1.13	0.28	1.47	1.24

XC240×240×8-B240×240×8	1.0	1.00	30	2.37	2.51	0.31	1.36	2.15	0.33	0.02	1.64	1.47
XC240×240×8-B400×240×8	1.0	1.00	30	2.18	2.27	0.28	1.27	2.01	0.30	0.03	1.32	1.23
XC400×240×8-B240×240×8	1.0	1.00	30	2.43	2.67	0.77	1.67	2.35	0.33	0.01	1.58	1.47
XC400×240×8-B400×240×8	1.0	1.00	30	2.29	2.45	0.56	1.52	2.22	0.31	0.00	1.29	1.24
XC120×120×4-B80×120×8	1.0	2.00	30	3.75	4.61	1.16	1.02	0.94	0.13	0.23	3.16	3.81
XC120×120×4-B240×120×8	1.0	2.00	30	3.37	3.94	1.18	0.90	0.96	0.19	0.32	2.55	1.79
XC200×120×4-B80×120×8	1.0	2.00	30	3.72	4.78	1.41	1.32	0.96	0.13	0.24	3.08	3.89
XC200×120×4-B240×120×8	1.0	2.00	30	3.57	4.40	1.22	1.06	1.07	0.19	0.27	2.45	1.91
XC120×200×4-B240×200×8	1.0	2.00	50	4.24	4.98	1.50	1.19	1.22	0.28	0.26	3.06	2.14
XC120×200×4-B400×200×8	1.0	2.00	50	3.95	4.64	1.41	1.16	1.19	0.30	0.31	2.58	1.47
XC200×200×4-B240×200×8	1.0	2.00	50	4.51	5.55	1.54	1.37	1.36	0.26	0.18	2.95	2.30
XC200×200×4-B400×200×8	1.0	2.00	50	4.18	5.17	1.47	1.29	1.30	0.29	0.23	2.65	1.80
XC180×300×6-B120×150×12	0.5	2.00	50	30.24	129.27	70.14	26.59	-0.96	-3.02	10.93	20.77	105.85
XC300×300×6-B120×150×12	0.5	2.00	50	31.94	137.76	73.02	24.89	-1.99	-3.76	9.22	22.00	113.01
XC180×300×6-B120×240×12	0.8	2.00	50	28.10	60.37	22.62	6.47	-2.08	-0.84	1.11	21.42	48.76
XC180×300×6-B360×240×12	0.8	2.00	50	29.48	58.09	24.33	8.07	-1.97	-0.19	1.68	15.92	23.07
XC300×300×6-B120×240×12	0.8	2.00	50	28.71	62.58	23.23	5.81	-2.55	-1.03	0.64	21.91	50.48
XC300×300×6-B360×240×12	0.8	2.00	50	30.51	61.59	25.40	7.41	-2.39	-0.38	1.19	16.12	25.26
XC180×180×6-B120×180×12	1.0	2.00	30	4.04	5.12	1.25	1.14	1.04	0.14	0.25	3.39	4.14
XC180×180×6-B360×180×12	1.0	2.00	30	3.37	4.07	1.18	0.95	1.00	0.21	0.33	2.55	1.84
XC300×180×6-B120×180×12	1.0	2.00	30	4.01	5.30	1.52	1.48	1.06	0.14	0.27	3.29	4.22
XC300×180×6-B360×180×12	1.0	2.00	30	3.59	4.54	1.22	1.11	1.11	0.21	0.28	2.45	1.94
XC180×300×6-B360×300×12	1.0	2.00	50	4.26	5.14	1.50	1.25	1.26	0.29	0.27	3.06	2.18
XC300×300×6-B360×300×12	1.0	2.00	50	4.53	5.72	1.54	1.45	1.41	0.28	0.18	2.95	2.34
XC160×160×16-B160×160×16	1.0	1.00	10	1.46	1.33	0.33	0.76	1.35	1.22	0.37	1.47	1.26
XC240×240×8-B160×240×16	1.0	2.00	30	4.03	5.21	1.24	1.20	1.05	0.15	0.26	3.38	4.19
XC400×240×8-B160×240×16	1.0	2.00	30	4.00	5.39	1.52	1.54	1.07	0.14	0.28	3.28	4.26

Table 7. SCFs of stainless steel tubular X-joints at typical hot spot locations obtained from finite element analysis

Specimen	SCF_{CIDECT}				$SCF_{Proposed}$					SCF_{FE}/SCF_{CIDECT}				$SCF_{FE}/SCF_{Proposed}$				
	A	B	C	D	A	B	C	D	H	A	B	C	D	A	B	C	D	H
XC120×200×4-B30×40×1	13.73	26.06	22.98	8.85	8.87	12.70	12.60	9.98	2.68	0.68	0.47	0.54	0.83	1.05	0.96	0.98	0.74	0.68
XC120×200×4-B50×40×1	13.73	26.06	22.98	8.85	8.87	12.70	12.60	9.98	2.68	0.94	0.59	0.67	1.03	1.45	1.20	1.21	0.91	0.54
XC200×200×4-B30×40×1	13.73	26.06	22.98	8.85	8.87	12.70	12.60	9.98	2.68	0.70	0.49	0.55	0.84	1.08	1.00	1.01	0.74	0.75
XC200×200×4-B50×40×1	13.73	26.06	22.98	8.85	8.87	12.70	12.60	9.98	2.68	0.98	0.62	0.69	1.04	1.52	1.27	1.27	0.93	0.58
XC60×60×2-B30×30×1	25.03	26.51	23.09	10.83	14.50	18.65	13.91	7.14	7.01	0.27	0.67	0.59	0.60	0.47	0.95	0.98	0.91	0.96
XC60×60×2-B50×30×1	25.03	26.51	23.09	10.83	14.50	18.65	13.91	7.14	7.01	0.32	0.76	0.68	0.69	0.54	1.08	1.12	1.05	0.80
XC100×60×2-B30×30×1	25.03	26.51	23.09	10.83	14.50	18.65	13.91	7.14	7.01	0.28	0.70	0.62	0.60	0.48	0.99	1.02	0.91	1.00
XC100×60×2-B50×30×1	25.03	26.51	23.09	10.83	14.50	18.65	13.91	7.14	7.01	0.33	0.81	0.71	0.69	0.57	1.15	1.18	1.05	0.84
XC60×100×2-B30×50×1	46.48	72.10	49.42	25.16	19.72	39.41	30.52	16.06	10.48	0.23	0.41	0.55	0.51	0.55	0.75	0.90	0.80	0.95
XC60×100×2-B50×50×1	46.48	72.10	49.42	25.16	19.72	39.41	30.52	16.06	10.48	0.29	0.50	0.68	0.63	0.69	0.92	1.10	0.99	1.01
XC100×100×2-B30×50×1	46.48	72.10	49.42	25.16	19.72	39.41	30.52	16.06	10.48	0.24	0.44	0.58	0.51	0.58	0.80	0.94	0.80	1.00
XC100×100×2-B50×50×1	46.48	72.10	49.42	25.16	19.72	39.41	30.52	16.06	10.48	0.31	0.54	0.72	0.64	0.73	0.99	1.16	1.01	1.07
XC30×50×1-B30×40×1	23.19	61.43	-26.46	19.08	17.84	31.15	16.83	6.93	10.33	0.31	0.36	-0.74	0.47	0.41	0.71	1.16	1.31	1.01
XC30×50×1-B50×40×1	23.19	61.43	-26.46	19.08	17.84	31.15	16.83	6.93	10.33	0.35	0.41	-0.84	0.56	0.45	0.80	1.33	1.53	0.75
XC50×50×1-B30×40×1	23.19	61.43	-26.46	19.08	17.84	31.15	16.83	6.93	10.33	0.32	0.39	-0.80	0.47	0.42	0.77	1.25	1.29	1.03
XC50×50×1-B50×40×1	23.19	61.43	-26.46	19.08	17.84	31.15	16.83	6.93	10.33	0.36	0.44	-0.91	0.55	0.47	0.88	1.44	1.52	0.77
XC40×40×4-B30×40×1	1.62	0.10	0.36	0.14	1.30	0.55	0.14	0.42	0.90	0.86	2.80	0.03	1.21	1.08	0.51	0.07	0.40	1.36
XC40×40×4-B50×40×1	1.62	0.10	0.36	0.14	1.30	0.55	0.14	0.42	0.90	0.83	3.10	0.06	1.57	1.04	0.56	0.14	0.52	1.18
XC30×30×1-B30×30×1	3.07	2.60	0.00	1.96	2.71	2.37	0.82	0.90	1.83	0.69	0.68	—	-0.28	0.78	0.75	0.34	0.61	0.89
XC30×30×1-B50×30×1	3.07	2.60	0.00	1.96	2.71	2.37	0.82	0.90	1.83	0.65	0.63	—	-0.26	0.74	0.70	0.30	0.57	0.73
XC50×30×1-B30×30×1	3.07	2.60	0.00	1.96	2.71	2.37	0.82	0.90	1.83	0.71	0.75	—	-0.25	0.80	0.82	0.98	0.54	0.85
XC50×30×1-B50×30×1	3.07	2.60	0.00	1.96	2.71	2.37	0.82	0.90	1.83	0.68	0.70	—	-0.26	0.77	0.76	0.71	0.56	0.70
XC30×50×1-B30×50×1	4.12	7.18	-48.67	4.08	3.10	2.80	0.90	1.07	1.83	0.65	0.36	-0.01	-0.17	0.86	0.93	0.34	0.66	1.09
XC30×50×1-B50×50×1	4.12	7.18	-48.67	4.08	3.10	2.80	0.90	1.07	1.83	0.62	0.29	-0.01	-0.17	0.83	0.75	0.29	0.64	0.89
XC50×50×1-B30×50×1	4.12	7.18	-48.67	4.08	3.10	2.80	0.90	1.07	1.83	0.67	0.34	-0.02	-0.16	0.88	0.87	1.01	0.61	1.05
XC50×50×1-B50×50×1	4.12	7.18	-48.67	4.08	3.10	2.80	0.90	1.07	1.83	0.65	0.32	-0.01	-0.16	0.87	0.83	0.66	0.63	0.86
XC120×200×4-B40×40×4	13.73	73.70	64.99	25.03	12.55	38.50	25.20	15.12	5.35	0.66	0.58	0.48	0.76	0.72	1.11	1.23	1.26	1.18
XC200×200×4-B40×40×4	13.73	73.70	64.99	25.03	12.55	38.50	25.20	15.12	5.35	0.70	0.61	0.49	0.75	0.76	1.17	1.28	1.25	1.26
XC160×160×16-B40×80×4	6.61	1.83	1.54	1.05	3.51	1.11	1.69	1.11	1.89	0.58	0.66	1.11	1.08	1.09	1.08	1.01	1.02	1.77

XC160×160×16-B120×80×4	6.61	1.83	1.54	1.05	3.51	1.11	1.69	1.11	1.89	0.68	0.80	1.37	1.26	1.28	1.32	1.25	1.19	0.88
XC80×80×8-B40×40×4	6.61	3.08	2.59	1.77	4.18	1.93	2.39	1.36	2.68	0.51	0.60	0.87	0.67	0.81	0.95	0.94	0.88	1.11
XC240×240×8-B120×120×4	25.03	26.51	23.09	10.83	14.50	18.65	13.91	7.14	7.01	0.80	0.86	0.78	0.84	1.38	1.22	1.29	1.27	0.95
XC240×240×8-B200×120×4	25.03	26.51	23.09	10.83	14.50	18.65	13.91	7.14	7.01	0.92	0.97	0.90	0.98	1.58	1.38	1.50	1.49	0.80
XC400×240×8-B120×120×4	25.03	26.51	23.09	10.83	14.50	18.65	13.91	7.14	7.01	0.83	0.90	0.81	0.83	1.43	1.27	1.34	1.26	0.99
XC400×240×8-B200×120×4	25.03	26.51	23.09	10.83	14.50	18.65	13.91	7.14	7.01	0.96	1.03	0.95	0.99	1.65	1.46	1.57	1.49	0.83
XC120×120×4-B40×60×4	25.03	44.58	38.83	18.22	17.25	32.47	19.67	8.79	9.91	0.43	0.69	0.41	0.37	0.62	0.95	0.81	0.77	0.86
XC120×120×4-B120×60×4	25.03	44.58	38.83	18.22	17.25	32.47	19.67	8.79	9.91	0.60	0.79	0.52	0.52	0.87	1.08	1.03	1.08	0.87
XC200×120×4-B40×60×4	25.03	44.58	38.83	18.22	17.25	32.47	19.67	8.79	9.91	0.44	0.72	0.42	0.35	0.64	0.99	0.84	0.73	0.89
XC200×120×4-B120×60×4	25.03	44.58	38.83	18.22	17.25	32.47	19.67	8.79	9.91	0.62	0.83	0.54	0.51	0.90	1.14	1.07	1.05	0.90
XC120×200×4-B120×100×4	46.48	121.26	83.12	42.31	23.45	68.61	43.17	19.77	14.83	0.61	0.56	0.56	0.52	1.21	0.99	1.08	1.12	1.13
XC120×200×4-B200×100×4	46.48	121.26	83.12	42.31	23.45	68.61	43.17	19.77	14.83	0.70	0.64	0.64	0.60	1.39	1.13	1.22	1.29	1.13
XC200×200×4-B120×100×4	46.48	121.26	83.12	42.31	23.45	68.61	43.17	19.77	14.83	0.65	0.60	0.59	0.52	1.28	1.06	1.13	1.10	1.20
XC200×200×4-B200×100×4	46.48	121.26	83.12	42.31	23.45	68.61	43.17	19.77	14.83	0.75	0.69	0.68	0.61	1.49	1.22	1.31	1.30	1.19
XC60×100×2-B40×50×4	46.48	203.94	139.79	71.16	27.88	119.46	61.05	24.34	20.97	0.35	0.55	0.45	0.35	0.58	0.93	1.03	1.03	0.62
XC100×100×2-B40×50×4	46.48	203.94	139.79	71.16	27.88	119.46	61.05	24.34	20.97	0.37	0.58	0.47	0.33	0.61	0.99	1.07	0.97	0.65
XC120×200×4-B120×160×4	23.19	61.43	-26.46	19.08	17.84	31.15	16.83	6.93	10.33	1.02	0.54	-0.74	0.46	1.33	1.06	1.16	1.26	1.01
XC120×200×4-B200×160×4	23.19	61.43	-26.46	19.08	17.84	31.15	16.83	6.93	10.33	1.15	0.60	-0.83	0.53	1.49	1.19	1.31	1.45	0.76
XC200×200×4-B120×160×4	23.19	61.43	-26.46	19.08	17.84	31.15	16.83	6.93	10.33	1.05	0.57	-0.76	0.45	1.37	1.12	1.20	1.23	1.03
XC200×200×4-B200×160×4	23.19	61.43	-26.46	19.08	17.84	31.15	16.83	6.93	10.33	1.20	0.65	-0.87	0.52	1.56	1.27	1.36	1.43	0.78
XC60×100×2-B40×80×4	23.19	103.31	-44.51	32.09	21.22	54.23	23.80	8.53	14.61	0.61	0.39	-0.49	0.21	0.67	0.74	0.92	0.77	0.86
XC60×100×2-B120×80×4	23.19	103.31	-44.51	32.09	21.22	54.23	23.80	8.53	14.61	0.70	0.40	-0.56	0.27	0.77	0.76	1.04	1.02	0.73
XC100×100×2-B40×80×4	23.19	103.31	-44.51	32.09	21.22	54.23	23.80	8.53	14.61	0.62	0.41	-0.52	0.19	0.68	0.78	0.97	0.72	0.88
XC100×100×2-B120×80×4	23.19	103.31	-44.51	32.09	21.22	54.23	23.80	8.53	14.61	0.73	0.43	-0.60	0.26	0.79	0.82	1.12	0.96	0.74
XC160×160×16-B120×160×4	1.62	0.10	0.36	0.14	1.30	0.55	0.14	0.42	0.90	0.88	3.50	-0.03	2.36	1.10	0.64	0.07	0.79	1.37
XC160×160×16-B200×160×4	1.62	0.10	0.36	0.14	1.30	0.55	0.14	0.42	0.90	0.83	3.80	0.11	2.64	1.03	0.69	0.29	0.88	1.18
XC80×80×8-B40×80×4	1.62	0.17	0.60	0.24	1.55	0.95	0.20	0.52	1.28	0.96	4.47	0.47	1.21	1.01	0.80	1.40	0.56	1.20
XC80×80×8-B120×80×4	1.62	0.17	0.60	0.24	1.55	0.95	0.20	0.52	1.28	0.81	4.47	0.40	1.50	0.85	0.80	1.20	0.69	0.84
XC40×40×4-B40×40×4	1.62	0.29	1.00	0.41	1.84	1.66	0.28	0.63	1.81	0.89	4.21	0.33	0.44	0.78	0.73	1.18	0.29	0.81
XC120×120×4-B120×120×4	3.07	2.60	0.00	1.96	2.71	2.37	0.82	0.90	1.83	0.76	0.87	—	0.45	0.86	0.95	0.38	0.99	0.89
XC120×120×4-B200×120×4	3.07	2.60	0.00	1.96	2.71	2.37	0.82	0.90	1.83	0.70	0.79	—	0.42	0.80	0.86	0.34	0.92	0.72

XC200×120×4-B120×120×4	3.07	2.60	0.00	1.96	2.71	2.37	0.82	0.90	1.83	0.78	0.93	—	0.57	0.89	1.02	0.93	1.24	0.86
XC200×120×4-B200×120×4	3.07	2.60	0.00	1.96	2.71	2.37	0.82	0.90	1.83	0.74	0.85	—	0.52	0.84	0.94	0.68	1.13	0.70
XC120×200×4-B120×200×4	4.12	7.18	-48.67	4.08	3.10	2.80	0.90	1.07	1.83	0.74	0.40	-0.01	0.29	0.99	1.03	0.42	1.10	1.14
XC120×200×4-B200×200×4	4.12	7.18	-48.67	4.08	3.10	2.80	0.90	1.07	1.83	0.68	0.36	-0.01	0.27	0.91	0.94	0.34	1.04	0.89
XC200×200×4-B120×200×4	4.12	7.18	-48.67	4.08	3.10	2.80	0.90	1.07	1.83	0.76	0.43	-0.02	0.36	1.01	1.11	1.01	1.38	1.10
XC200×200×4-B200×200×4	4.12	7.18	-48.67	4.08	3.10	2.80	0.90	1.07	1.83	0.72	0.40	-0.01	0.33	0.95	1.02	0.67	1.24	0.87
XC60×60×2-B40×60×4	3.07	4.37	0.00	3.30	3.23	4.13	1.17	1.11	2.59	1.21	1.00	—	0.29	1.15	1.05	1.03	0.86	1.25
XC60×60×2-B120×60×4	3.07	4.37	0.00	3.30	3.23	4.13	1.17	1.11	2.59	1.06	0.83	—	0.25	1.01	0.88	1.02	0.73	0.98
XC100×60×2-B40×60×4	3.07	4.37	0.00	3.30	3.23	4.13	1.17	1.11	2.59	1.20	1.03	—	0.38	1.14	1.09	1.25	1.12	1.21
XC100×60×2-B120×60×4	3.07	4.37	0.00	3.30	3.23	4.13	1.17	1.11	2.59	1.13	0.93	—	0.29	1.07	0.98	1.05	0.87	0.95
XC60×100×2-B120×100×4	4.12	12.08	-81.86	6.86	3.69	4.87	1.28	1.31	2.58	1.00	0.38	-0.02	0.15	1.11	0.94	1.16	0.81	1.19
XC60×100×2-B200×100×4	4.12	12.08	-81.86	6.86	3.69	4.87	1.28	1.31	2.58	0.93	0.35	-0.02	0.15	1.04	0.88	1.10	0.79	1.00
XC100×100×2-B120×100×4	4.12	12.08	-81.86	6.86	3.69	4.87	1.28	1.31	2.58	1.06	0.42	-0.02	0.18	1.18	1.05	1.20	0.95	1.14
XC100×100×2-B200×100×4	4.12	12.08	-81.86	6.86	3.69	4.87	1.28	1.31	2.58	0.98	0.39	-0.02	0.17	1.10	0.98	1.16	0.89	1.03
XC160×160×16-B80×80×8	6.61	3.08	2.59	1.77	4.18	1.93	2.39	1.36	2.68	0.75	0.60	0.66	0.98	1.19	0.95	0.72	1.27	1.46
XC240×240×8-B80×120×8	25.03	44.58	38.83	18.22	17.25	32.47	19.67	8.79	9.91	0.62	0.78	0.50	0.42	0.90	1.07	0.98	0.86	1.12
XC240×240×8-B240×120×8	25.03	44.58	38.83	18.22	17.25	32.47	19.67	8.79	9.91	0.85	0.88	0.64	0.59	1.23	1.21	1.26	1.22	1.09
XC400×240×8-B80×120×8	25.03	44.58	38.83	18.22	17.25	32.47	19.67	8.79	9.91	0.64	0.81	0.51	0.40	0.92	1.11	1.01	0.82	1.16
XC400×240×8-B240×120×8	25.03	44.58	38.83	18.22	17.25	32.47	19.67	8.79	9.91	0.88	0.93	0.67	0.57	1.28	1.28	1.31	1.18	1.13
XC120×200×4-B80×100×8	46.48	203.94	139.79	71.16	27.88	119.46	61.05	24.34	20.97	0.54	0.61	0.49	0.37	0.90	1.05	1.11	1.08	0.84
XC200×200×4-B80×100×8	46.48	203.94	139.79	71.16	27.88	119.46	61.05	24.34	20.97	0.57	0.65	0.51	0.35	0.95	1.11	1.16	1.01	0.89
XC120×200×4-B80×160×8	23.19	103.31	-44.51	32.09	21.22	54.23	23.80	8.53	14.61	0.87	0.51	-0.44	0.19	0.95	0.98	0.82	0.70	1.07
XC120×200×4-B240×160×8	23.19	103.31	-44.51	32.09	21.22	54.23	23.80	8.53	14.61	1.04	0.56	-0.54	0.26	1.13	1.07	1.01	0.99	0.92
XC200×200×4-B80×160×8	23.19	103.31	-44.51	32.09	21.22	54.23	23.80	8.53	14.61	0.89	0.53	-0.45	0.17	0.97	1.02	0.83	0.62	1.09
XC200×200×4-B240×160×8	23.19	103.31	-44.51	32.09	21.22	54.23	23.80	8.53	14.61	1.07	0.60	-0.55	0.24	1.17	1.13	1.04	0.91	0.93
XC160×160×16-B80×160×8	1.62	0.17	0.60	0.24	1.55	0.95	0.20	0.52	1.28	0.95	4.76	0.45	1.92	0.99	0.85	1.35	0.88	1.19
XC160×160×16-B240×160×8	1.62	0.17	0.60	0.24	1.55	0.95	0.20	0.52	1.28	0.81	5.00	0.40	2.25	0.85	0.89	1.20	1.04	0.84
XC80×80×8-B80×80×8	1.62	0.29	1.00	0.41	1.84	1.66	0.28	0.63	1.81	0.90	4.45	0.33	1.17	0.79	0.78	1.18	0.76	0.81
XC240×240×8-B240×240×8	3.07	2.60	0.00	1.96	2.71	2.37	0.82	0.90	1.83	0.77	0.97	—	0.69	0.87	1.06	0.38	1.51	0.90
XC240×240×8-B400×240×8	3.07	2.60	0.00	1.96	2.71	2.37	0.82	0.90	1.83	0.71	0.87	—	0.65	0.80	0.96	0.34	1.41	0.72
XC400×240×8-B240×240×8	3.07	2.60	0.00	1.96	2.71	2.37	0.82	0.90	1.83	0.79	1.03	—	0.85	0.90	1.13	0.94	1.86	0.86

XC400×240×8-B400×240×8	3.07	2.60	0.00	1.96	2.71	2.37	0.82	0.90	1.83	0.75	0.94	—	0.78	0.85	1.03	0.68	1.69	0.70
XC120×120×4-B80×120×8	3.07	4.37	0.00	3.30	3.23	4.13	1.17	1.11	2.59	1.22	1.05	—	0.31	1.16	1.12	0.99	0.92	1.22
XC120×120×4-B240×120×8	3.07	4.37	0.00	3.30	3.23	4.13	1.17	1.11	2.59	1.10	0.90	—	0.27	1.04	0.95	1.01	0.81	0.98
XC200×120×4-B80×120×8	3.07	4.37	0.00	3.30	3.23	4.13	1.17	1.11	2.59	1.21	1.09	—	0.40	1.15	1.16	1.21	1.19	1.19
XC200×120×4-B240×120×8	3.07	4.37	0.00	3.30	3.23	4.13	1.17	1.11	2.59	1.16	1.01	—	0.32	1.11	1.07	1.04	0.95	0.95
XC120×200×4-B240×200×8	4.12	12.08	-81.86	6.86	3.69	4.87	1.28	1.31	2.58	1.03	0.41	-0.02	0.17	1.15	1.02	1.17	0.91	1.19
XC120×200×4-B400×200×8	4.12	12.08	-81.86	6.86	3.69	4.87	1.28	1.31	2.58	0.96	0.38	-0.02	0.17	1.07	0.95	1.10	0.89	1.00
XC200×200×4-B240×200×8	4.12	12.08	-81.86	6.86	3.69	4.87	1.28	1.31	2.58	1.09	0.46	-0.02	0.20	1.22	1.14	1.20	1.05	1.14
XC200×200×4-B400×200×8	4.12	12.08	-81.86	6.86	3.69	4.87	1.28	1.31	2.58	1.01	0.43	-0.02	0.19	1.13	1.06	1.15	0.98	1.03
XC180×300×6-B120×150×12	46.48	203.94	139.79	71.16	27.88	119.46	61.05	24.34	20.97	0.65	0.63	0.50	0.37	1.08	1.08	1.15	1.09	0.99
XC300×300×6-B120×150×12	46.48	203.94	139.79	71.16	27.88	119.46	61.05	24.34	20.97	0.69	0.68	0.52	0.35	1.15	1.15	1.20	1.02	1.05
XC180×300×6-B120×240×12	23.19	103.31	-44.51	32.09	21.22	54.23	23.80	8.53	14.61	1.21	0.58	-0.51	0.20	1.32	1.11	0.95	0.76	1.47
XC180×300×6-B360×240×12	23.19	103.31	-44.51	32.09	21.22	54.23	23.80	8.53	14.61	1.27	0.56	-0.55	0.25	1.39	1.07	1.02	0.95	1.09
XC300×300×6-B120×240×12	23.19	103.31	-44.51	32.09	21.22	54.23	23.80	8.53	14.61	1.24	0.61	-0.52	0.18	1.35	1.15	0.98	0.68	1.50
XC300×300×6-B360×240×12	23.19	103.31	-44.51	32.09	21.22	54.23	23.80	8.53	14.61	1.32	0.60	-0.57	0.23	1.44	1.14	1.07	0.87	1.10
XC180×180×6-B120×180×12	3.07	4.37	0.00	3.30	3.23	4.13	1.17	1.11	2.59	1.32	1.17	—	0.35	1.25	1.24	1.07	1.03	1.31
XC180×180×6-B360×180×12	3.07	4.37	0.00	3.30	3.23	4.13	1.17	1.11	2.59	1.10	0.93	—	0.29	1.04	0.99	1.01	0.86	0.98
XC300×180×6-B120×180×12	3.07	4.37	0.00	3.30	3.23	4.13	1.17	1.11	2.59	1.31	1.21	—	0.45	1.24	1.28	1.30	1.33	1.27
XC300×180×6-B360×180×12	3.07	4.37	0.00	3.30	3.23	4.13	1.17	1.11	2.59	1.17	1.04	—	0.34	1.11	1.10	1.04	1.00	0.95
XC180×300×6-B360×300×12	4.12	12.08	-81.86	6.86	3.69	4.87	1.28	1.31	2.58	1.03	0.43	-0.02	0.18	1.15	1.06	1.17	0.95	1.19
XC300×300×6-B360×300×12	4.12	12.08	-81.86	6.86	3.69	4.87	1.28	1.31	2.58	1.10	0.47	-0.02	0.21	1.23	1.17	1.20	1.11	1.14
XC160×160×16-B160×160×16	1.62	0.29	1.00	0.41	1.84	1.66	0.28	0.63	1.81	0.90	4.59	0.33	1.85	0.79	0.80	1.18	1.21	0.81
XC240×240×8-B160×240×16	3.07	4.37	0.00	3.30	3.23	4.13	1.17	1.11	2.59	1.31	1.19	—	0.36	1.25	1.26	1.06	1.08	1.31
XC400×240×8-B160×240×16	3.07	4.37	0.00	3.30	3.23	4.13	1.17	1.11	2.59	1.30	1.23	—	0.47	1.24	1.31	1.30	1.39	1.27
Mean										0.80	0.99	0.17	0.54	1.00	1.00	1.00	1.00	1.00
COV										0.350	1.069	3.071	0.932	0.281	0.177	0.316	0.279	0.211

Table 8. Comparison of SCFs predicted by finite element analysis with SCFs calculated using CIDECT design formulae and proposed unified design equation

Comparison	Hot spot location		Coefficient							
			a	*b*	*c*	*d*	*e*	*f*	*g*	*h*
Current design rules	Brace	A/E	0.013	0.693	-0.278	0	0.790	1.898	-2.109	0
		Joints with fillet welds	SCF_A and SCF_E are multiplied by a factor of 1.40 for brace side of weld.							
	Chord	B	0.143	-0.204	0.064	0	1.377	1.715	-1.103	0.75
		C	0.077	-0.129	0.061	-0.0003	1.565	1.874	-1.028	0.75
		D	0.208	-0.387	0.209	0	0.925	2.389	-1.881	0.75
		X-joints (β=1.0)	SCF_C is multiplied by a factor of 0.65; SCF_D is multiplied by a factor of 0.50.							
Proposed design rules	Brace	A/E/F	0.725	-2.000	2.000	-0.0025	0.270	4.350	-4.200	0.250
		H	1.700	-5.000	5.000	-0.0015	-0.250	4.480	-4.200	0.500
	Chord	B/I	0.191	-1.276	1.856	-0.0002	4.288	-3.800	-0.155	0.800
		C	0.015	0.250	-0.250	-0.0002	1.500	0.778	-0.950	0.500
		D/G	0.075	-0.300	0.540	0.0003	1.200	1.800	-2.700	0.300

Table 9. Comparison of current design formulae with proposed design equation for SCFs of tubular X-joints at typical hot spot locations

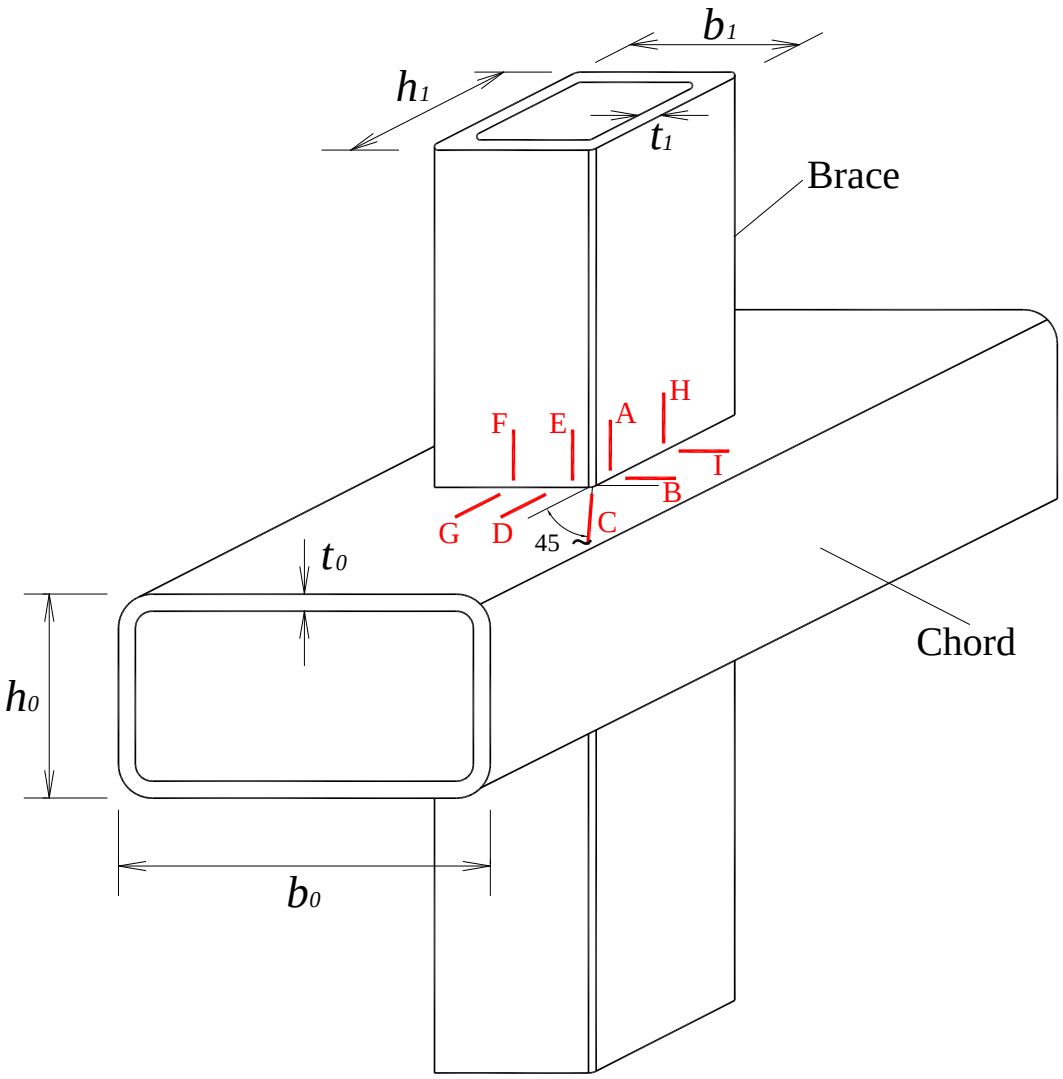

Figure 1. Typical hot spot locations of stainless steel tubular X-joint

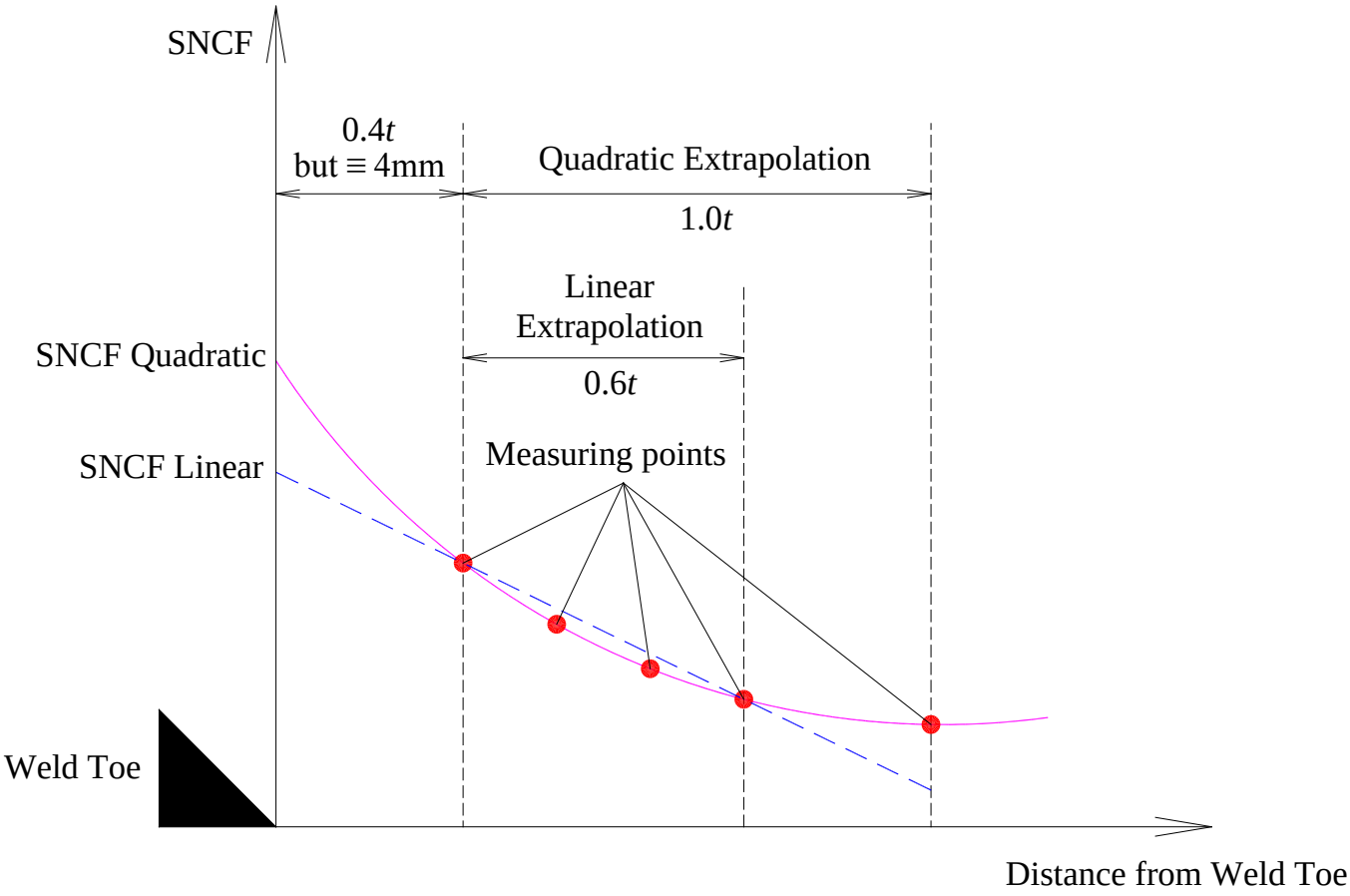

Figure 2. Methods of extrapolation to the weld toe

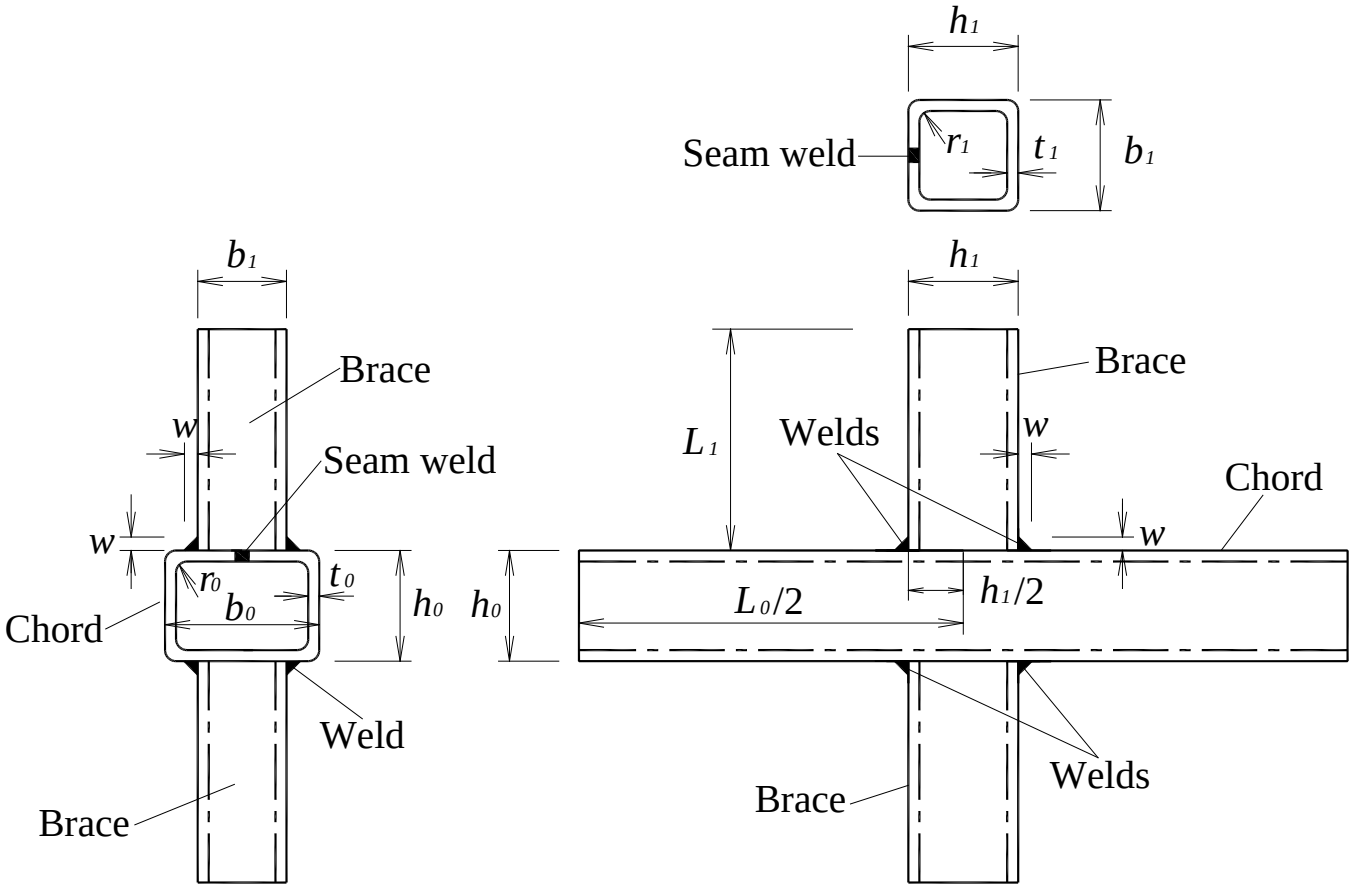

(a) End view (b) Elevation

Figure 3. Definition of symbols for stainless steel tubular X-joint

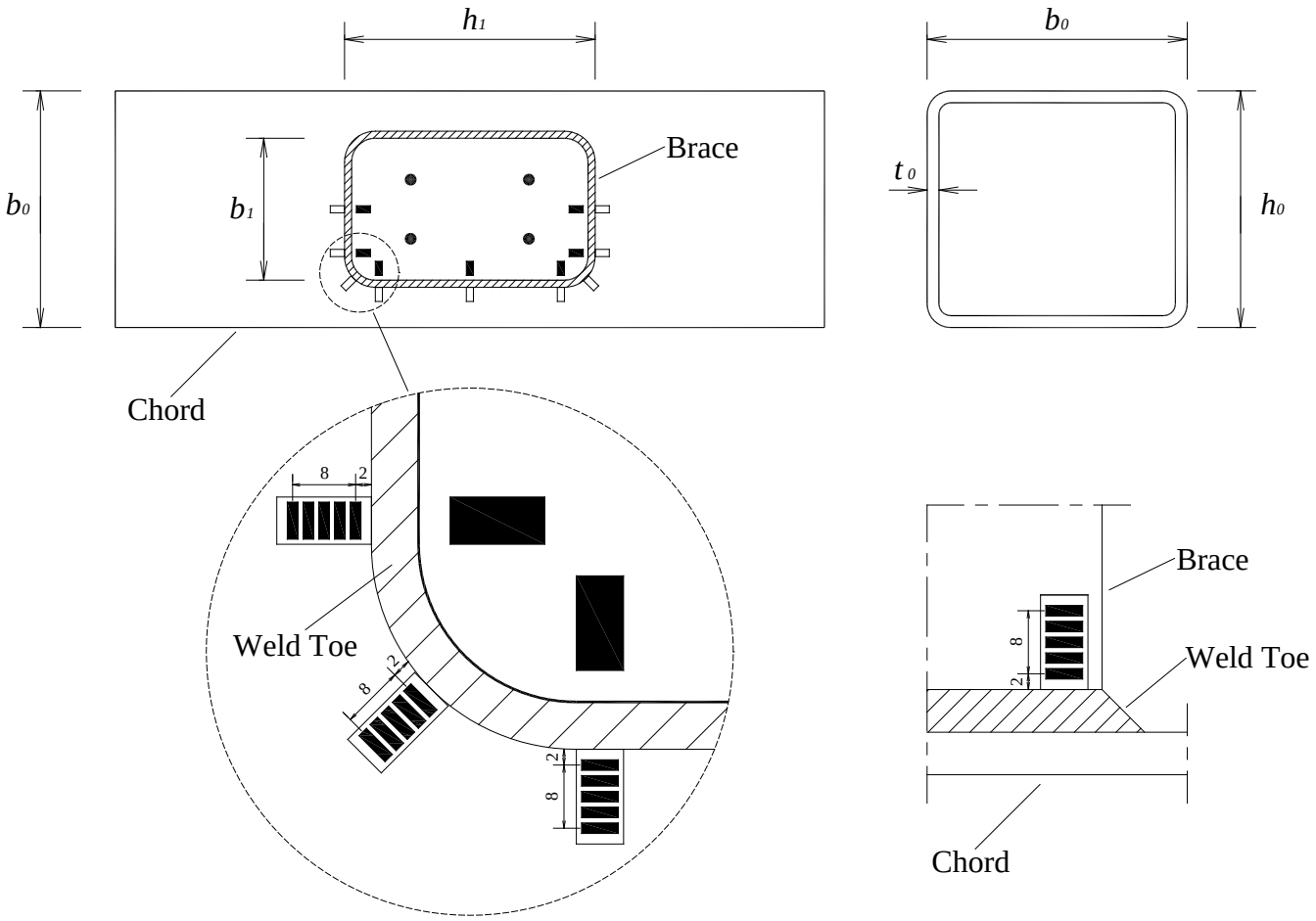

- ● : Single element strain gauge for nominal strain at mid-length of brace member
- ▭ : Strip strain gauges for hot spot strain (HSSN) at chord member
- ▬ : Strip strain gauges for hot spot strain (HSSN) at brace member

Figure 4. Location of strain gauges

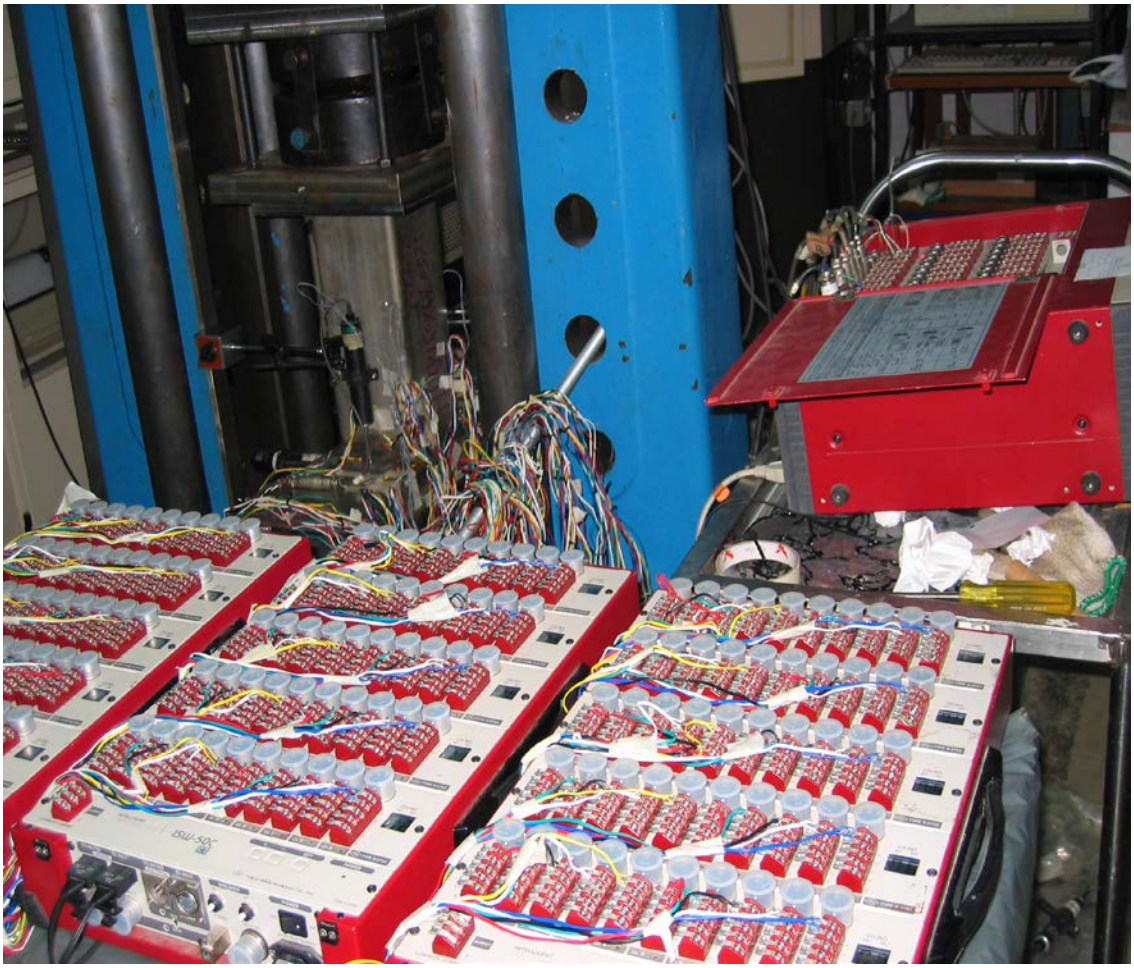

Figure 5. Typical test setup for SCFs of stainless steel tubular X-joint

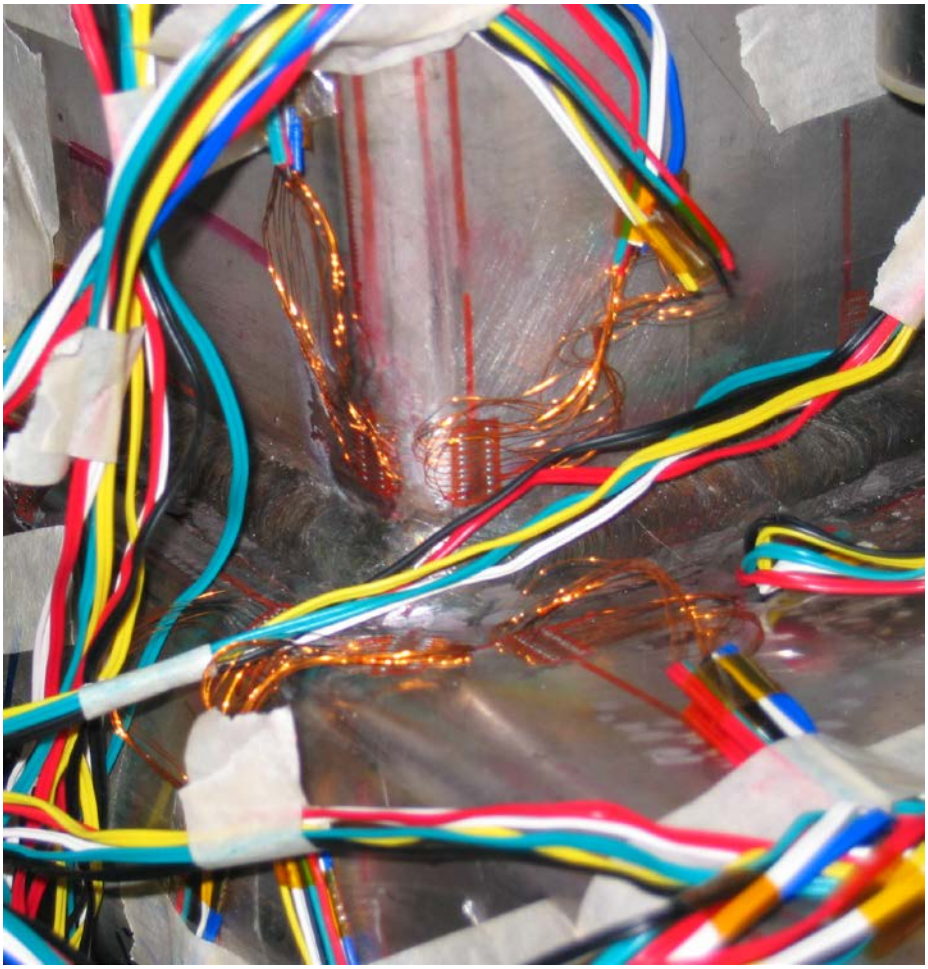

Figure 6. A close up view of the strip strain gauges specific to stress concentration measurements of stainless steel tubular X-joint

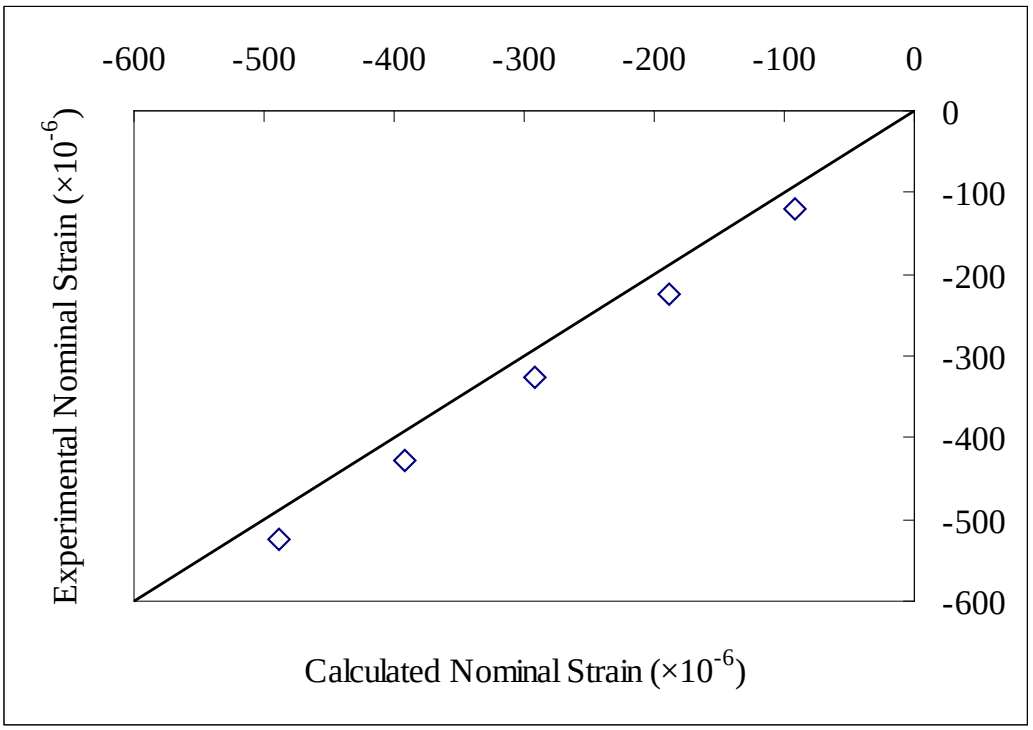

Figure 7. Experimental nominal strain versus calculated nominal strain for stainless steel tubular X-joint of specimen XD-C140×3-B40×2

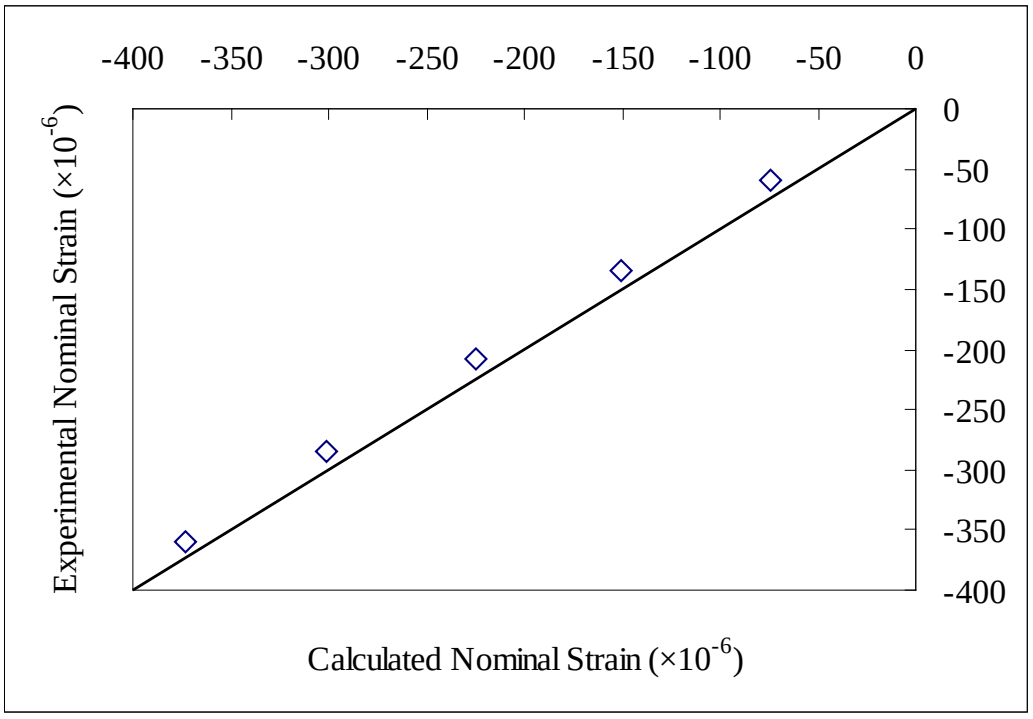

Figure 8. Experimental nominal strain versus calculated nominal strain for stainless steel tubular X-joint of specimen XD-C140×3-B140×3

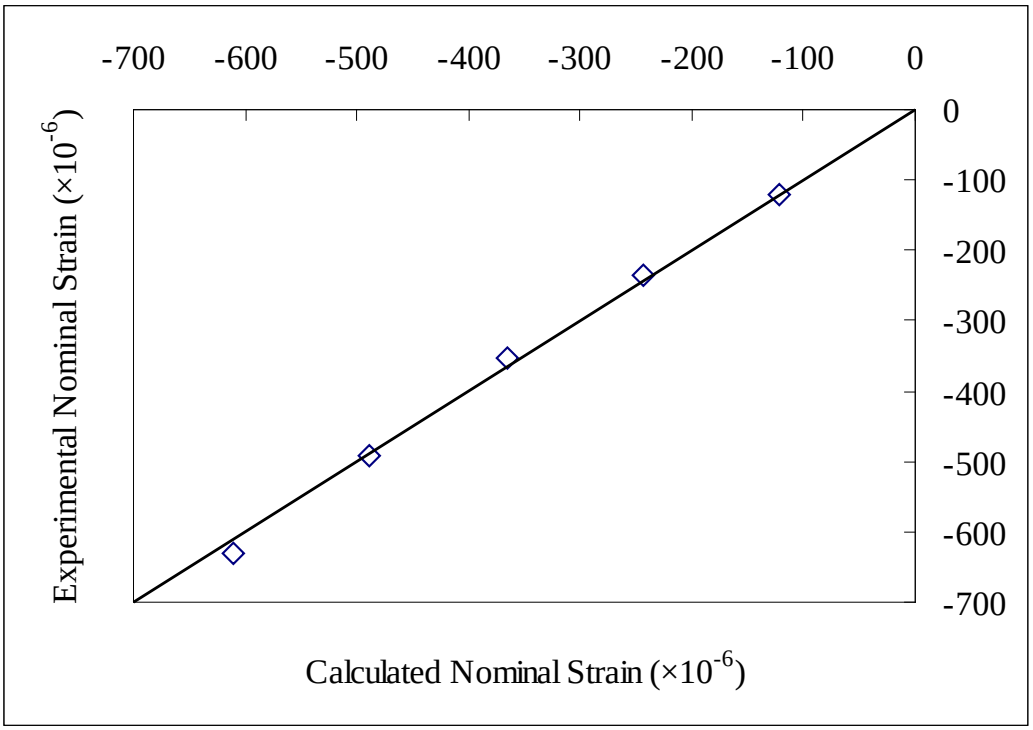

Figure 9. Experimental nominal strain versus calculated nominal strain for stainless steel tubular X-joint of specimen XH-C150×6-B150×6

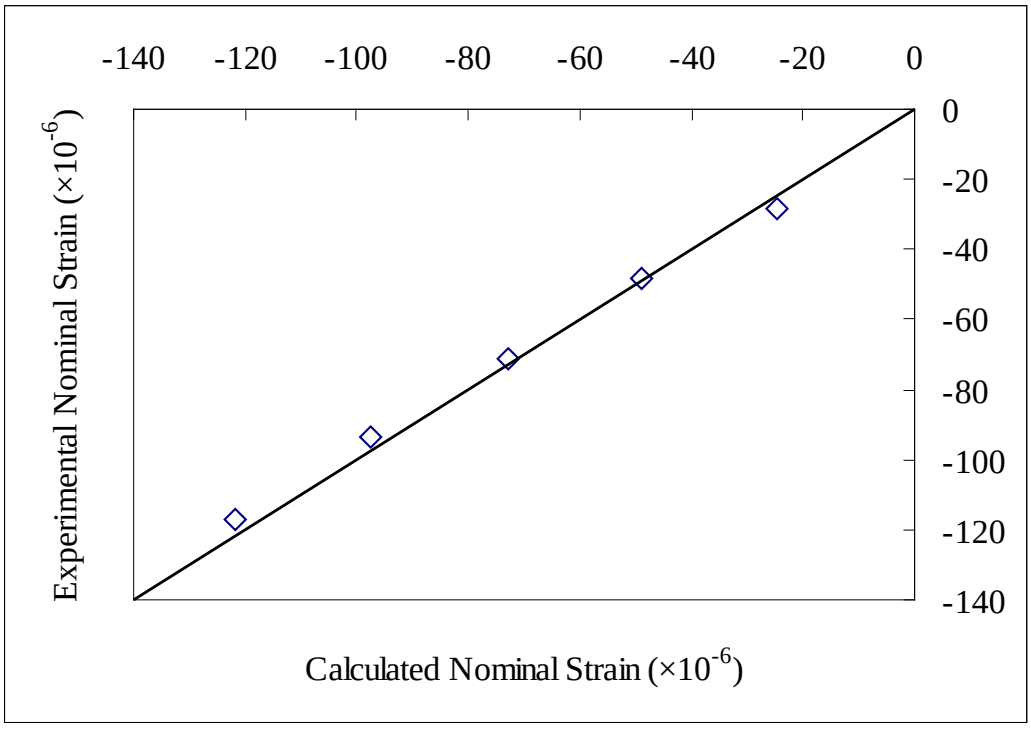

Figure 10. Experimental nominal strain versus calculated nominal strain for stainless steel tubular X-joint of specimen XH-C110×4-B150×6

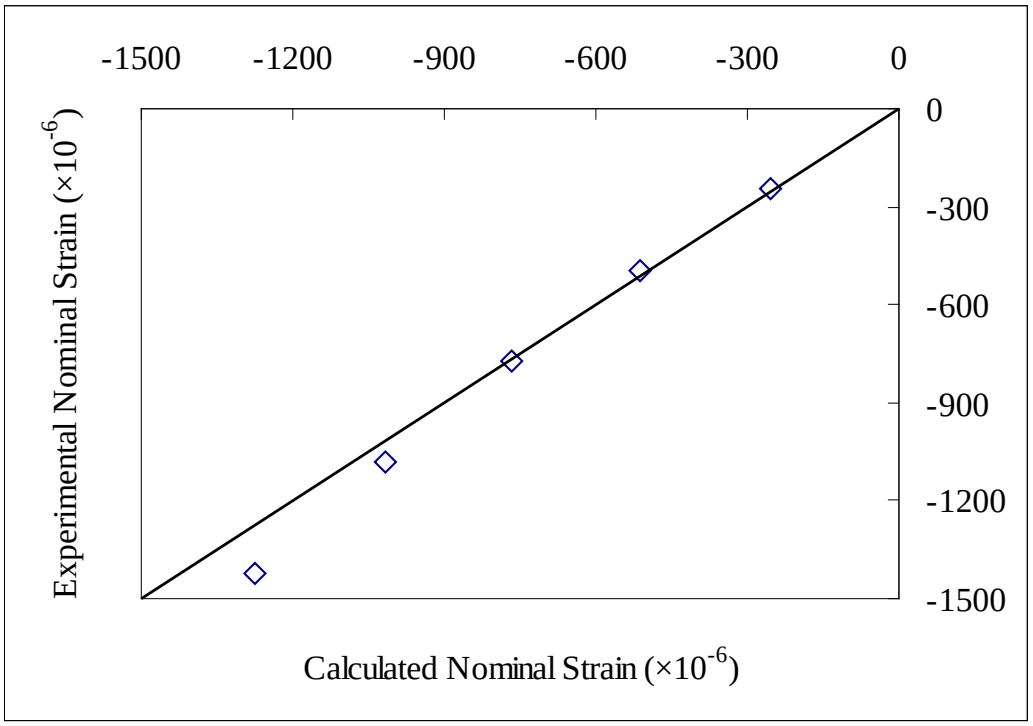

Figure 11. Experimental nominal strain versus calculated nominal strain for stainless steel tubular X-joint of specimen XN-C40×4-B40×2

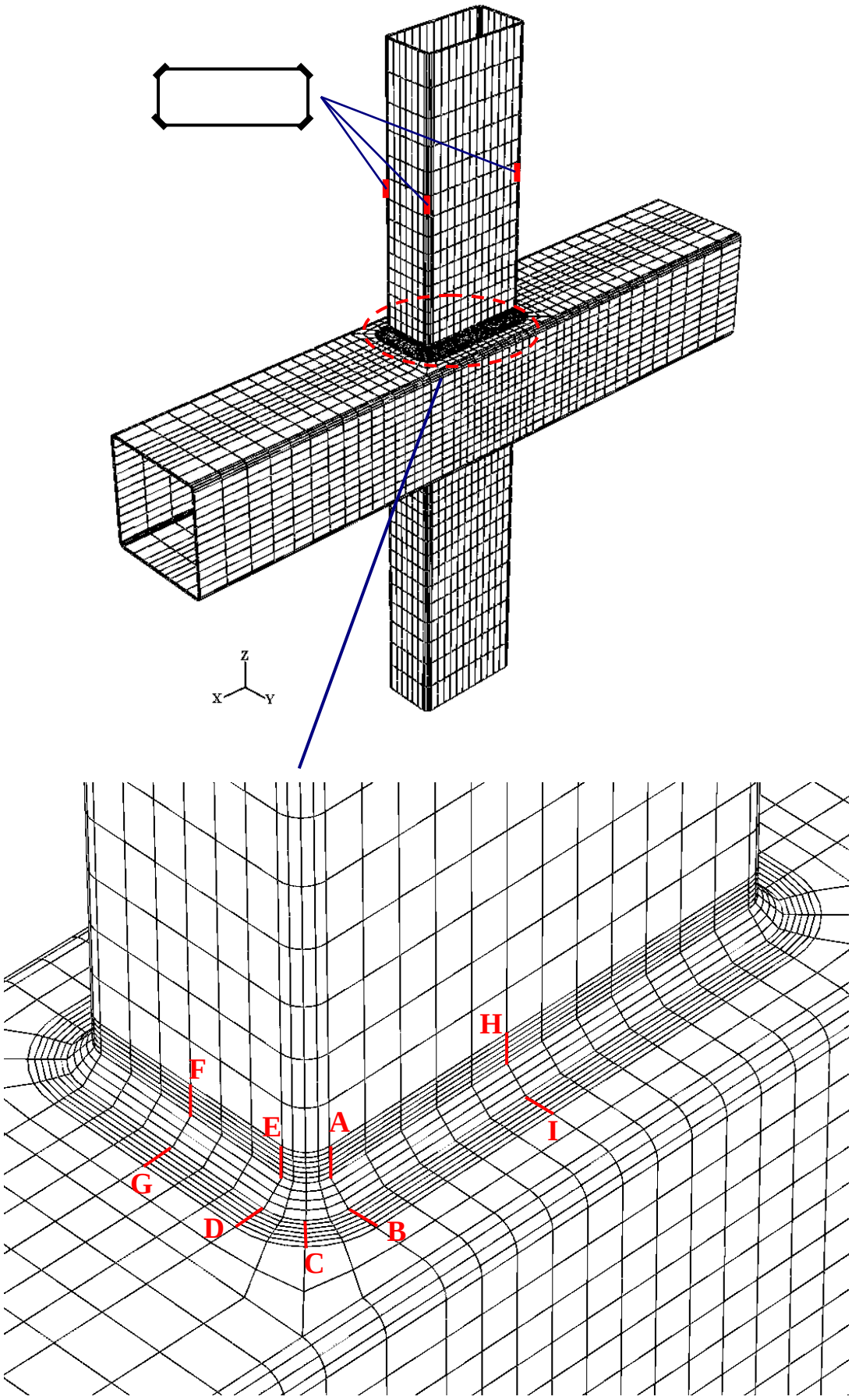

Figure 12. Typical details of hot spot locations in finite element model